Groundwater-Flow Model for the Wood River Valley Aquifer System, Version 1.1

Idaho Department of Water Resources
Allan Wylie, Jennifer Sukow, Mike McVay, and James Bartolino

Abstract

This report documents the design, development, and calibration of the Wood River Valley (WRV) Aquifer Model Version 1.1. The objective of this update to WRV Aquifer Model 1.0 was to include data collected between 1/1/2011 and 12/31/2014 while preserving the basic design of the groundwater model developed by Fisher and others (2016). The geologic interpretations, groundwater-flow system understanding, and model layering and grid remain as described by Fisher. The model boundary was adjusted to include three additional irrigation wells.

The calibration data include river gain and loss records calculated using nine continuous gages. Three of the gages are on the Big Wood River, four of the gages measure tributary inflow to the Big Wood River and two measure discharge from springs that arise within the model boundary. Aquifer water-level data include 1,314 water-levels collected in 332 wells.

Adjustable parameters for the WRV Aquifer Model calibration include aquifer transmissivity, storage coefficient, riverbed conductance, drain conductance, irrigation efficiency, and tributary-aquifer underflow.

The calibration period (1/1/1998 through 12/31/2014) includes some of the wettest and driest years on record, indicating that the stresses the model is calibrated to include the range of stresses that can realistically be expected for most analyses. The fit between field observations and model output is good, suggesting that the model reasonably represents the hydrogeologic system.

Along with adding four additional years of data to the model period, the recalibration resulted in an improved representation of the length of the Big Wood River that becomes dry during the summer and the length of time it remains dry annually.

The length of the Big Wood River in hydrologic communication with the aquifer varies substantially during most years, making development of a numerical-superposition model inadvisable.

Keywords:

Aquifer river interaction, MODFLOW-USG, PEST, METRIC

Acknowledgements

The Idaho Department of Water Resources (IDWR) would like to thank the Idaho Water Resource Board for funding this project and for their guidance throughout the project. We also thank the Modeling Technical Advisory Group (MTAC) for their participation, input, and local insight.

Introduction

This report documents the design, development, and calibration of Wood River Valley (WRV) Aquifer Model Version 1.1. The objective of the WRV Aquifer Model Version 1.1 project was to include data collected between 1/1/2011 and 12/31/2014 with the original calibration period of 1/1/1998 through 12/31/2010 while updating the Wood River Valley aquifer model developed by Fisher and others (2016). Adding the years between 1/1/2011 and 12/31/2014 incorporates years during which more groundwater level and streamflow data were collected in the WRV than in any other four-year span in the calibration period. During this period the U.S. Geological Survey (USGS) conducted a mass measurement of wells in the WRV, conducted three seepage surveys on the Big Wood River and Silver Creek, and installed stream gages on the Big Wood River and four tributary streams. In addition, The IDWR installed pressure transducers in several wells, and significantly increased the number of wells routinely measured in the valley.

Descriptions of the study area, groundwater-flow system, and groundwater-flow model can be found in Fisher and others (2016). The geologic interpretations, the groundwater-flow system understanding, and the model layering and grid size used in WRV Aquifer Model Version 1.0 remain unchanged.

The boundary of the model was adjusted to include three irrigation wells near the Sportsman's Access Gage on Silver Creek. The added areas are within the circles in Figure 1.

The intent of this project is to update and improve upon the WRV Aquifer Model Version 1.0 calibration by including more years with higher data density while preserving the basic design of the model developed by Fisher and others (2016).

Model Development

WRV Aquifer Model Version 1.1 was calibrated using PEST (Doherty, 2016), an automated parameter estimation program. The goal of WRV model calibration is to adjust aquifer parameters within reasonable ranges until model-generated aquifer head, and gains to the Big Wood River, Willow Creek and Silver Creek match observed values. The adjustable parameters included riverbed conductance, drain conductance, irrigation-entity efficiency, tributary underflow, aquifer transmissivity, and aquifer storage. Transmissivity and aquifer storage were estimated using the PEST pilot points system (Doherty, 2003). PEST was only allowed to adjust parameters between assumed uncertainty bounds. For example, PEST could only adjust layer-one storage coefficients between 0.10 and 0.30 because those were assumed to be reasonable bounds based on available geologic information. Groundwater flow was simulated using MODFLOW-USG (Panday and others, 2013), a numerical model for simulating three-dimensional, steady-state and transient groundwater flow. Because the model is run many times during the parameter-estimation process, it was necessary to limit model run times. Substantial savings in model run times were achieved by simulating transient flow in the WRV aquifer system using a specified saturated thickness.

The following sections describe the parameter-estimation tools used for the WRV Aquifer Model calibration, as well as the observation data. Final model parameters and a comparison between model-predicted values and observed values are discussed in the subsequent "Model Calibration" section.

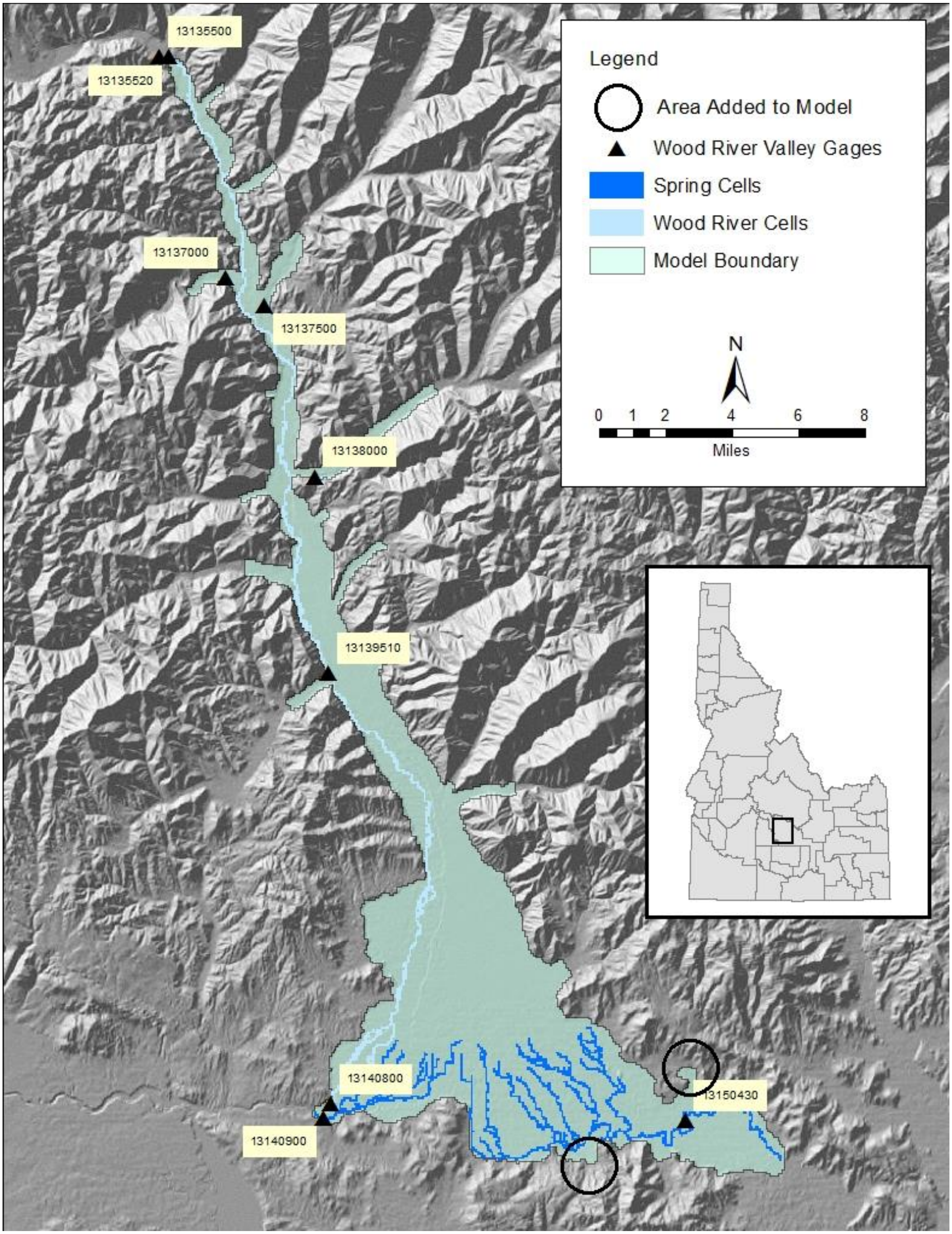

Figure 1. Location map and continuous river gages.

Parameter estimation tools

PEST, a nonlinear, least-squares inverse modeling program (Doherty, 2016) was used to calibrate the WRV Aquifer Model Version 1.1. During calibration, PEST runs MODFLOW-USG thousands of times, comparing model-generated values with field observations. The goal is to minimize the weighted, sum of the squared residuals, or difference between the model-generated values and the field observations.

River gain and loss data

River-gain and loss data consist of river-gaging information used to calculate gains from the aquifer to the river or losses from the river to the aquifer along the Big Wood River, Willow Creek, and Silver Creek and its tributaries. Streamflow measurements are available from the following nine continuous recording stations (Figure 1):

1. Big Wood River near Ketchum (USGS 13135500),
2. North Fork Big Wood River near Sawtooth NRA Headquarters (USGS 13135520),
3. Warm Springs Creek near Ketchum (USGS 13137000),
4. Trail Creek at Ketchum (USGS 13137500),
5. East Fork Big Wood River at Gimlet (USGS 13138000),
6. Big Wood River at Hailey (USGS 13139510),
7. Big Wood River at Stanton Crossing (USGS 13140800),
8. Willow Creek near Spring Creek Ranch (IPCO 13140900), and
9. Silver Creek at Sportsman Access (USGS 13150430).

Although most of these gages were not in operation during the entire model period, correlations with the gage at Hailey allow calculation of streamflow for the entire model period for Big Wood River near Ketchum, North Fork Big Wood River at Sawtooth NRA Headquarters, Warm Springs Creek near Ketchum, Trail Creek at Ketchum, and East Fork Big Wood River at Gimlet (Sukow, 2014). Semi-annual gaging of Silver Creek near Picabo (Wylie, 2019) and historic seepage surveys (Moreland, 1977) indicates that the gains between Sportsman Access and the model boundary are negligible. Thus the gages allow calculation of average monthly reach gains for five river reaches:

1. Big Wood River near Ketchum to at Hailey (240 observations between 1995-2015),
2. Big Wood River at Hailey to Stanton Crossing (219 observations between 1996-2015),
3. Willow Creek (173 observations between 2000-2015),
4. Silver Creek above Sportsman Access (240 observations between 1995-2015), and
5. Silver Creek Sportsman Access to Model Boundary (negligible based on a few streamflow measurements.

The USGS conducted three seepage surveys of the Big Wood River and Silver Creek. Each survey consisted of a single measurement at 28 different streamflow and diversion sites within the model domain. The seepage surveys were conducted in August 2012, October 2012, and March 2013

(Bartolino, 2014). Although each of the seepage surveys represent a single moment in time, they were conducted during the model-calibration period, and can be used to calculate reach gains and losses for shorter subreaches of the Big Wood River and Silver Creek.

Aquifer water level data

The calibration targets include water-levels collected by the USGS, IDWR, other cooperators, and water-well drillers. These measurements include mass measurements collected during October 2006 and October 2012. A total of 1,314 water-level measurements collected in 332 different wells were used in the model calibration. These observations fall into two categories:

1) Observation Well measurements. Measurements collected in wells with multiple water-level measurements (1,101 water-levels in 119 wells) (Figure 2), and
2) Geolocated Well measurements. Measurements obtained from driller logs (213 water-level measurements). The corresponding wells either have a GPS location provided by the driller or were geolocated using an addresses provided for the well by the driller (Figure 2).

Evapotranspiration

Evapotranspiration (ET), the sum of evaporation and plant transpiration, is a significant component of aquifer discharge in the WRV. Traditional ET estimation methods such as the FAO Penman-Monteith method (Allen and others, 1998) proved unreliable in the WRV because the county crop mix was not representative of the crops grown in the WRV. Therefore, ET for the WRV model was estimated using remote sensing techniques. Using ET estimates based on the METRIC algorithm (Allen and others, 2010) circumvented most of the problem. Where METRIC estimates for ET were not available for a model irrigation season, ET was estimated using Normalized Difference Vegetative Index (NDVI) (Allen and others, 2010). NDVI is a normalized ratio of the difference between red and infrared wavelengths reflected from the earth’s surface and serves as an indicator of viable plant cover. ET is strongly dependent on the presence of growing plants, enabling the development of strong correlations between NDVI and ET (McVay, 2014).

Model Calibration

Model calibration involves adjustment of model parameters to minimize the difference between model output and field observations. This section describes the adjustable parameters and the results. For the WRV Aquifer Model Version 1.1, the simulation period extends from 1/1/1995 through 12/31/2014 and the calibration period extends from 1/1/1998 through 12/31/2014. The period 1/1/1995 through 12/31/1997 provides the model with a three year warm-up before matching model output with field observations.

Transient calibration procedure

Each calibration iteration consisted of: first running the WRV water budget tool (Fisher and others, 2016), which calculates net recharge and writes a MODFLOW-USG well file, and then running MODFLOW-USG to calculate aquifer heads and aquifer-stream exchanges. Starting heads for each transient MODFLOW-USG simulation are calculated during an initial steady-state stress period. The well file for the initial steady-state stress period is generated using average water-budget data from April 2004 through March 2005. The steady-state stress period is used only to generate starting heads for the

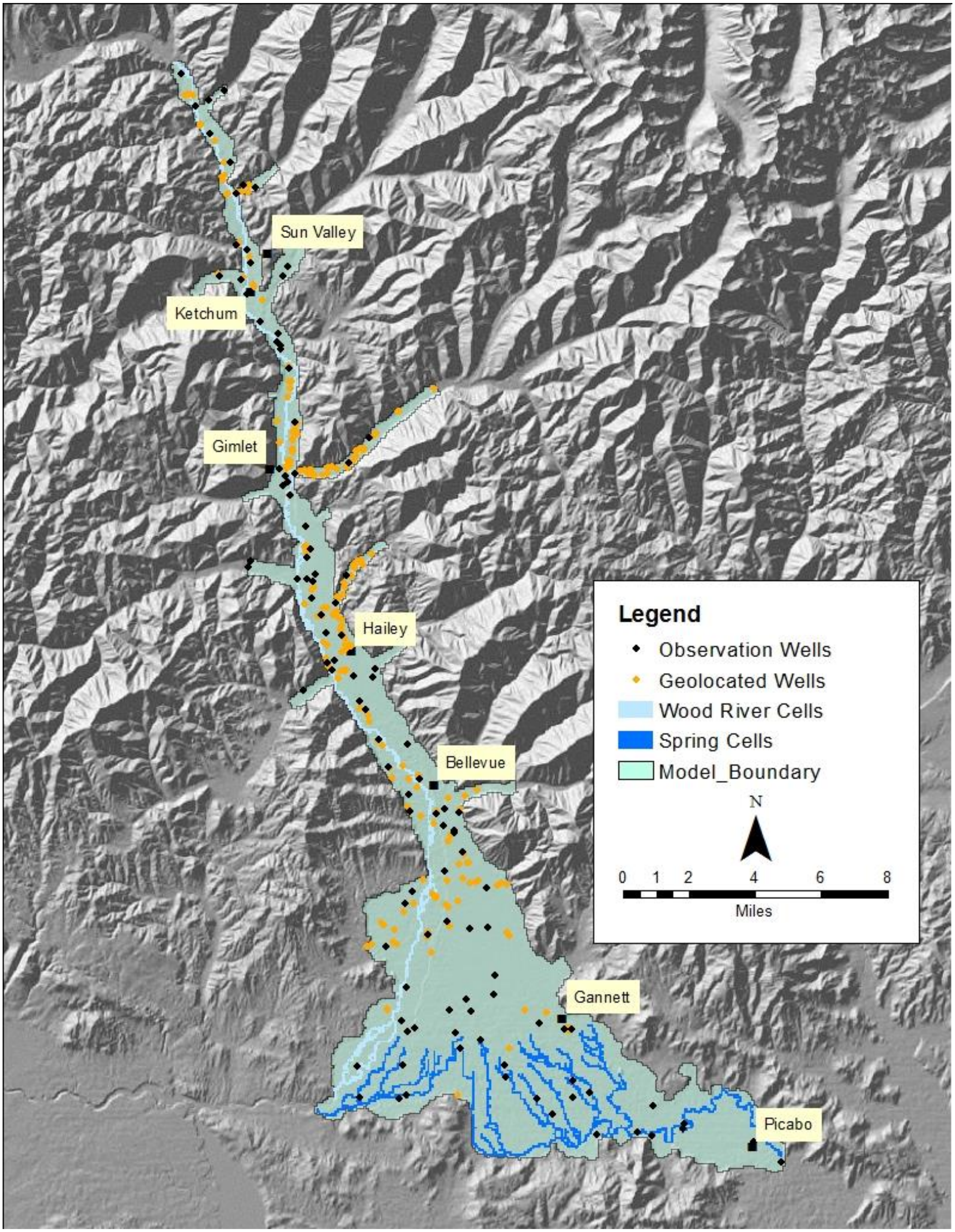

Figure 2. Observation and geolocated wells.

transient simulation. The model has a three-year warm-up period to recover from inaccuracies in the starting head field. PEST does not begin attempting to match modeled output with field observations until 1/1/1998. PEST adjusts recharge parameters as well as aquifer properties. The Modeling Technical Advisory Committee (MTAC) agreed to adjustment, within the bounds of uncertainty, on two of the components of recharge during model calibration. Adjustable components include irrigation-entity efficiency and tributary underflow. Irrigation entity efficiency describes what percentage of water diverted by an irrigation entity is consumptively used by crops. Tributary underflow is water entering the modeled aquifer system as groundwater from an adjacent aquifer.

Irrigation entity efficiency

An irrigation efficiency was assigned to all 89 irrigation entities. Conveyance losses were subtracted from the diverted volume before calculating entity efficiency for those entities with extensive canals (Figure 3). The lower and upper bounds for irrigation efficiency were set at 50% and 90%. Exceptions were made for entities the MTAC felt might benefit from natural sub-irrigation and for entities where water-measurement data indicated that entity efficiency could be outside the original bounds.

Tributary underflow

Prescribed-flux boundaries were used to represent tributary underflow for the major tributary valleys. Figure 4 shows the location of the 23 modeled tributary-underflow boundaries. Each tributary was assigned an initial long-term average underflow estimate as described in Appendix E of Fisher and others (2016). Tributary underflow was adjustable through three parameters: 1) a scalar that is multiplied with the initial long-term average estimate, 2) a moving average time span, and 3) an amplitude-reduction factor. Each tributary has a unique initial underflow estimate and a unique adjustable scalar. The moving average time span and amplitude-reduction factor are global and apply to all tributary valleys. Thus the flux at each tributary is unique, however the annual cycle (i.e., moving average and amplitude-reduction factor) are the same for all tributaries. This simplification is necessary because the data density in the tributary valleys is insufficient to allow adjustment of three unique tributary-underflow parameters for each of the 23 tributary valleys. The lower bound for each tributary scalar was set to 0.01 and the upper bound was set to a factor that would yield a product equal to 20% of the average annual precipitation within the tributary basin. The table in Figure 4 shows the average annual precipitation volume in each tributary basin and the modeled average annual underflow.

Aquifer hydraulic conductivity

The aquifer hydraulic conductivity distribution was estimated using a pilot-point parameterization method (Doherty, 2003). Parameter values were estimated for 271 pilot points and interpolated to the centroid of each model cell within the active model grid. Layer-one and Layer-three are divided into zones. The Layer-one zones separate the tributary valleys from the WRV (zone 1), and the Layer-three zones separate the alluvial aquifer (zone 1) from the basalt (zone 2). Layer-two consists of one zone. The delineation of the boundary between the lacustrine sediments, the sand and gravel, and the basalt portions of Layer-two is accomplished during calibration. Figures 5a through 5c show the various zones. The zones were defined based on geologic interpretation of driller logs.

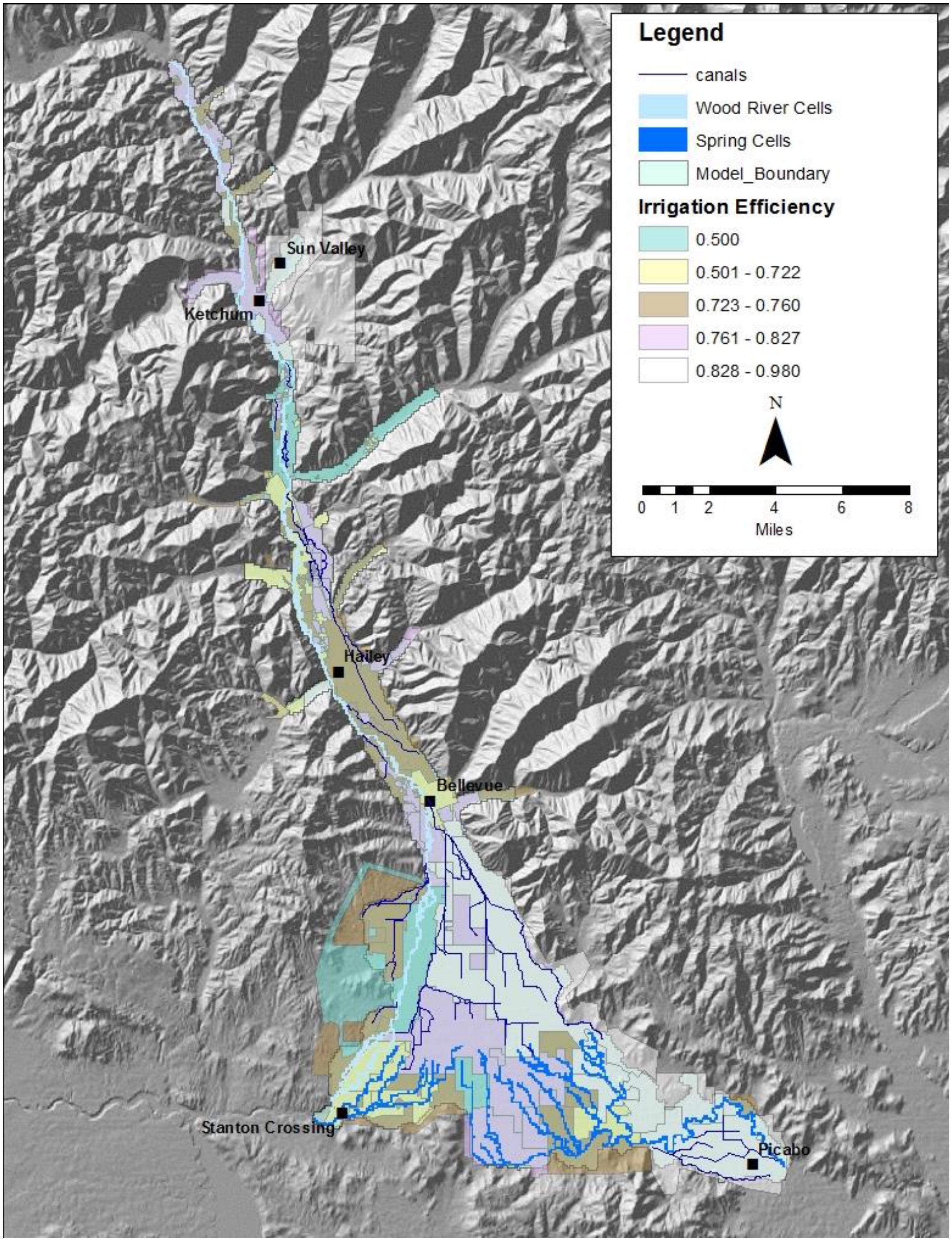

Figure 3. Irrigation entity efficiency.

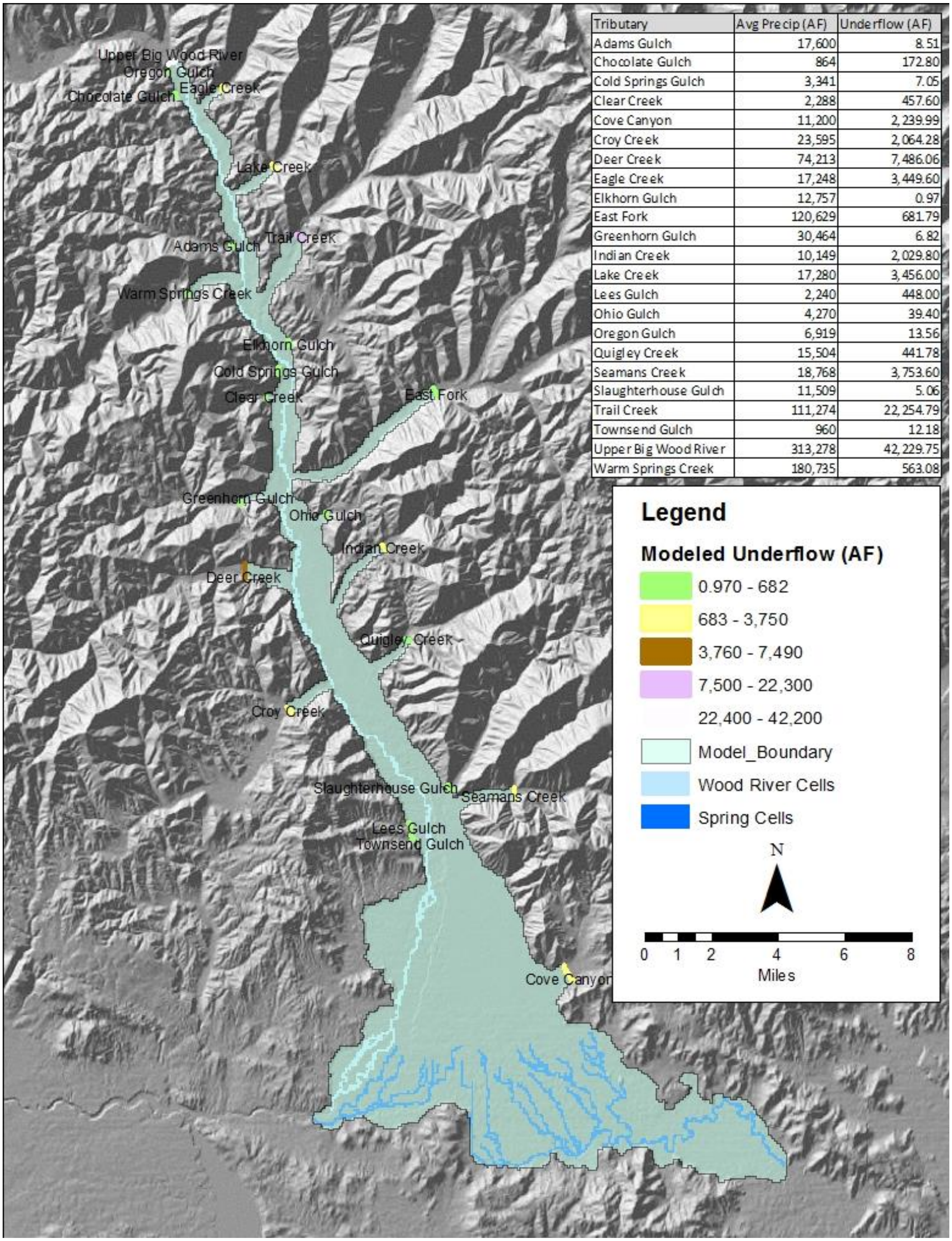

Tributary	Avg Precip (AF)	Underflow (AF)
Adams Gulch	17,600	8.51
Chocolate Gulch	864	172.80
Cold Springs Gulch	3,341	7.05
Clear Creek	2,288	457.60
Cove Canyon	11,200	2,239.99
Croy Creek	23,595	2,064.28
Deer Creek	74,213	7,486.06
Eagle Creek	17,248	3,449.60
Elkhorn Gulch	12,757	0.97
East Fork	120,629	681.79
Greenhorn Gulch	30,464	6.82
Indian Creek	10,149	2,029.80
Lake Creek	17,280	3,456.00
Lees Gulch	2,240	448.00
Ohio Gulch	4,270	39.40
Oregon Gulch	6,919	13.56
Quigley Creek	15,504	441.78
Seamans Creek	18,768	3,753.60
Slaughterhouse Gulch	11,509	5.06
Trail Creek	111,274	22,254.79
Townsend Gulch	960	12.18
Upper Big Wood River	313,278	42,229.75
Warm Springs Creek	180,735	563.08

Figure 4. Tributary underflow.

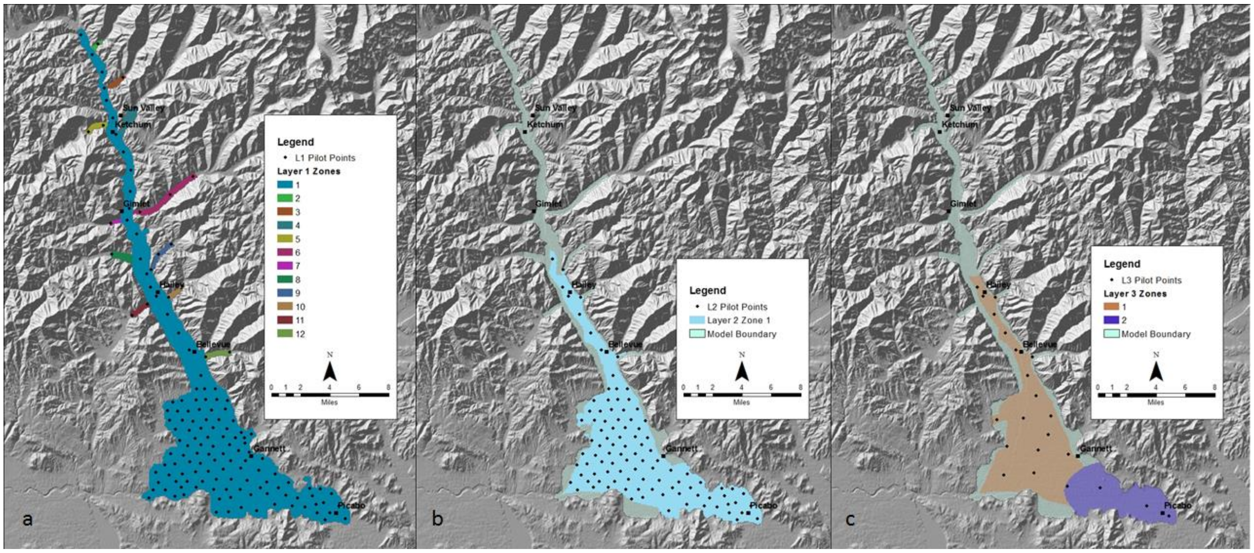

Figure 5. Hydraulic conductivity zones for Layers 1 (5a), 2 (5b), and 3 (5c).

Figures 6a through 6c show the calibrated hydraulic conductivity for Layer-one through Layer-three. Comparing Figure 3b from Fisher and others (2016) with Figure 6b in this document shows that for Layer-two, the calibration generally supports the delineation determined from the well logs. The major change is that calibration extends the lacustrine clays farther east toward Picabo. The resulting extent of the confining layer is consistent with earlier delineations of the confined aquifer (Moreland, 1977).

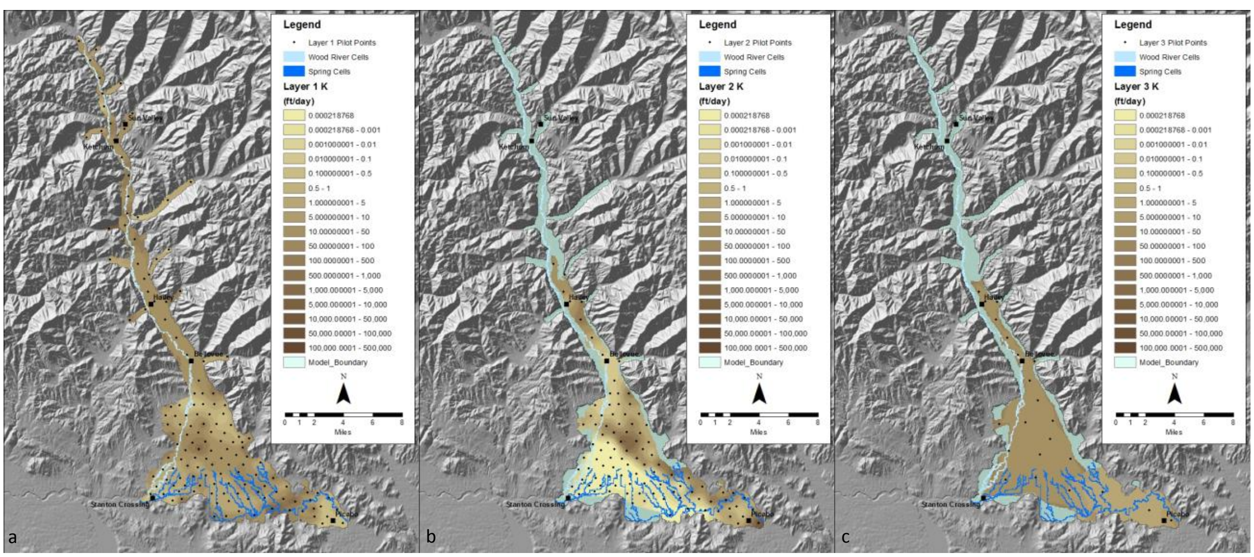

Figure 6. Calibrated hydraulic conductivity for Layers 1, 2, and 3.

Storage coefficient

The aquifer-storage coefficient distribution was calculated using a pilot-point parameterization method similar to the method used for the aquifer hydraulic conductivity distribution. The calibrated values are shown in Figures 7a through 7c.

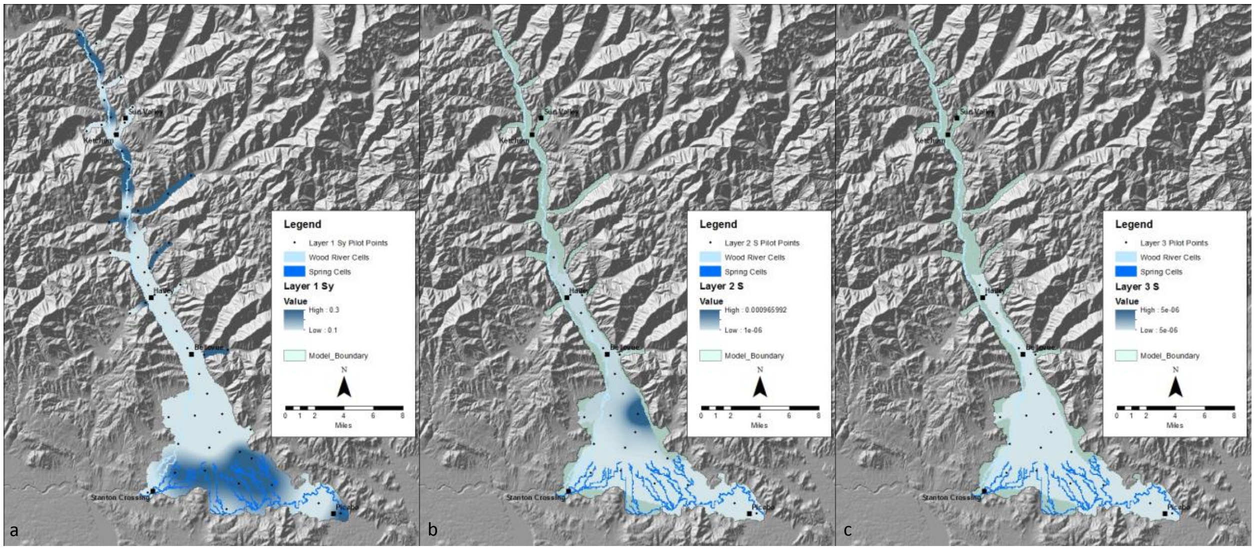

Figure 7. Calibrated aquifer storage coefficient for layers 1, 2, and 3, note that the color ramp is different for each layer.

All model layers were simulated using a fixed saturated thickness, so the storage coefficient for Layer-one is equivalent to a specific yield value. The calibrated storage coefficient values for Layer-one ranges from 0.10 to 0.30, consistent with literature estimates for alluvium (Freeze and Cherry, 1979). The calibrated values for Layers two and three range from 1.0e-6 to 9.7e-4.

Head-dependent river boundaries

Head-dependent boundaries are typically used to represent surface-water bodies which are hydraulically connected to an aquifer. Head-dependent boundaries include river boundaries, at which the flux may be either recharge or discharge from the aquifer, and drain boundaries, at which the flux may only be discharged from the aquifer (Panday and others, 2013). If the aquifer head in a river cell is above the water-surface elevation in the river (river stage), water flows from the aquifer into the river (aquifer discharge or river gain). If the aquifer head in a river cell is below the river stage, water enters the aquifer from the river (aquifer recharge or river loss).

For the purposes of this study, a river reach is a stretch of a river or stream defined by an upstream and downstream streamflow gage, or other means of determining flow. A subreach is a stretch of river or stream with an upstream and downstream measurement collected during one or more of the three seepage surveys conducted by the USGS during 2012 and 2013 (Bartolino, 2014). The Big Wood River, Silver Creek, and Willow Creek are represented by 2,551 river cells divided into five river reaches. The five river reaches (Figure 8a) are further subdivided into 21 subreaches (Figure 8b).

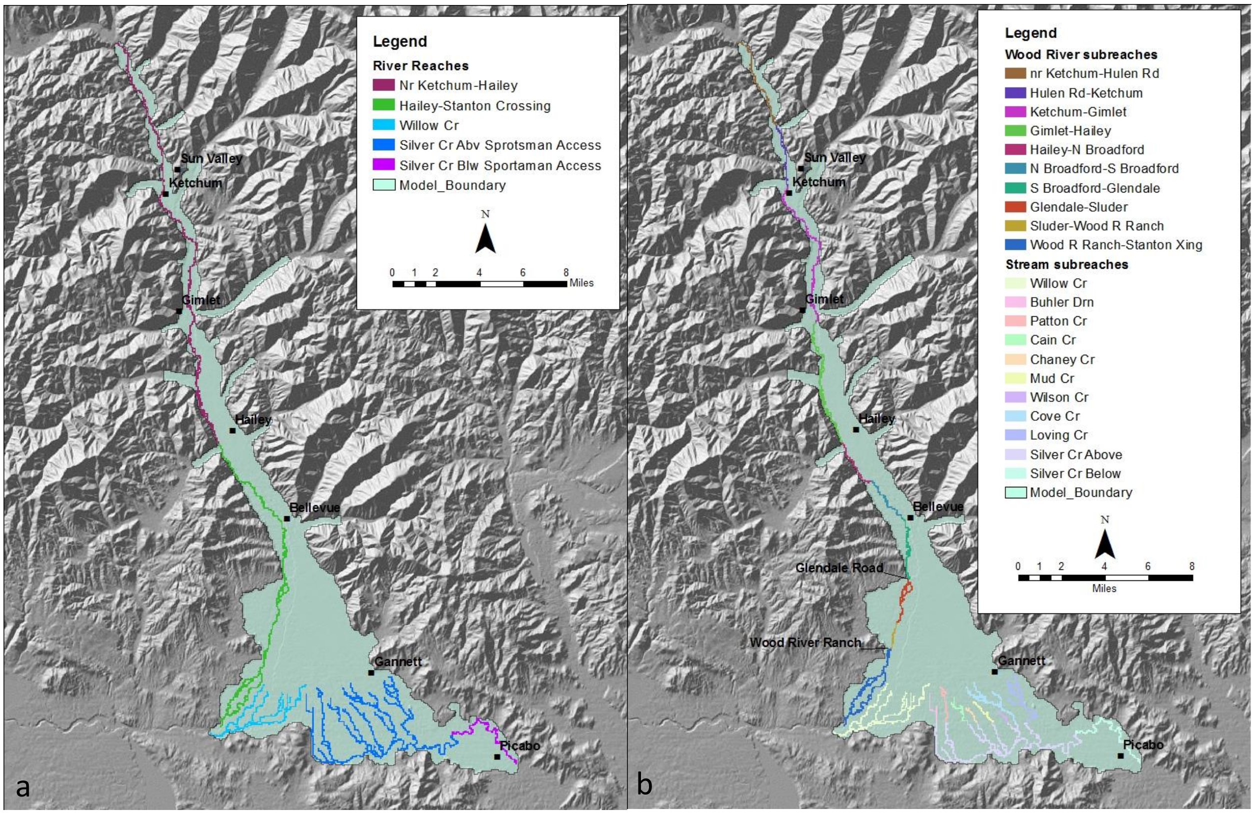

Figure 8. River reaches and subreaches.

River stage changes with each stress period along the Big Wood River. This is accomplished by interpolating between adjacent gages down to Glendale Road (Figure 8b). Landsat photos and water district records of priority cuts in surface-water rights are used to infer historical river conditions between Glendale Road and Stanton Crossing. When water district records indicate that the river was dry between Glendale Road and Wood River Ranch, river stage was set equal to the river bottom so the river head differential is zero and no water can leak from the river. When Landsat photos indicate water was flowing between Glendale Road and Wood River Ranch, river stage was set above the river bottom so water can seep from the river. When Landsat photos indicate that water is flowing between Wood River Ranch and Stanton Crossing, river stage is interpolated between Stanton Crossing and Wood River Ranch. When Landsat photos indicate that the river is dry, river stage is set equal to the river bottom.

The riverbed-conductance parameters are adjustable parameters that help govern seepage into and out of the river. Riverbed conductance is constant through time for most subreaches. The seepage from the river to the aquifer or from the aquifer to the river is a function of river stage, aquifer head, and riverbed conductance.

Generally, flow in a river is a function of stage in the river; the higher the stage, the higher the flow (Sanders, 1998). However, in the Glendale Road to Sluder Road and Sluder Road to Wood River Ranch subreaches, the river stage does not increase significantly as flow increases rather, the river spreads laterally. To approximate this phenomenon, different riverbed conductance parameters were provided when the average monthly river stage at Hailey exceeded certain values. When the average monthly river stage at Hailey was less than three feet, a riverbed-conductance term representing normal flow conditions was used; when the average monthly river stage exceeded three feet, a riverbed-conductance term representing high-flow conditions was used; and when the average monthly river stage exceeded 4.5 feet, a riverbed-conductance term representing especially high-flow conditions was used. Thus, there are three riverbed-conductance parameters used for the Glendale Road to Sluder Road subreach and three riverbed-conductance parameters use for the Sluder Road to Wood River Ranch subreach and the parameter that is used depends on the river stage recorded at the Hailey gage. Figure 1 shows the location of the gages, Figure 8b shows the location of the subreaches, and Figure 9 shows the recorded average monthly stage at the Hailey gage.

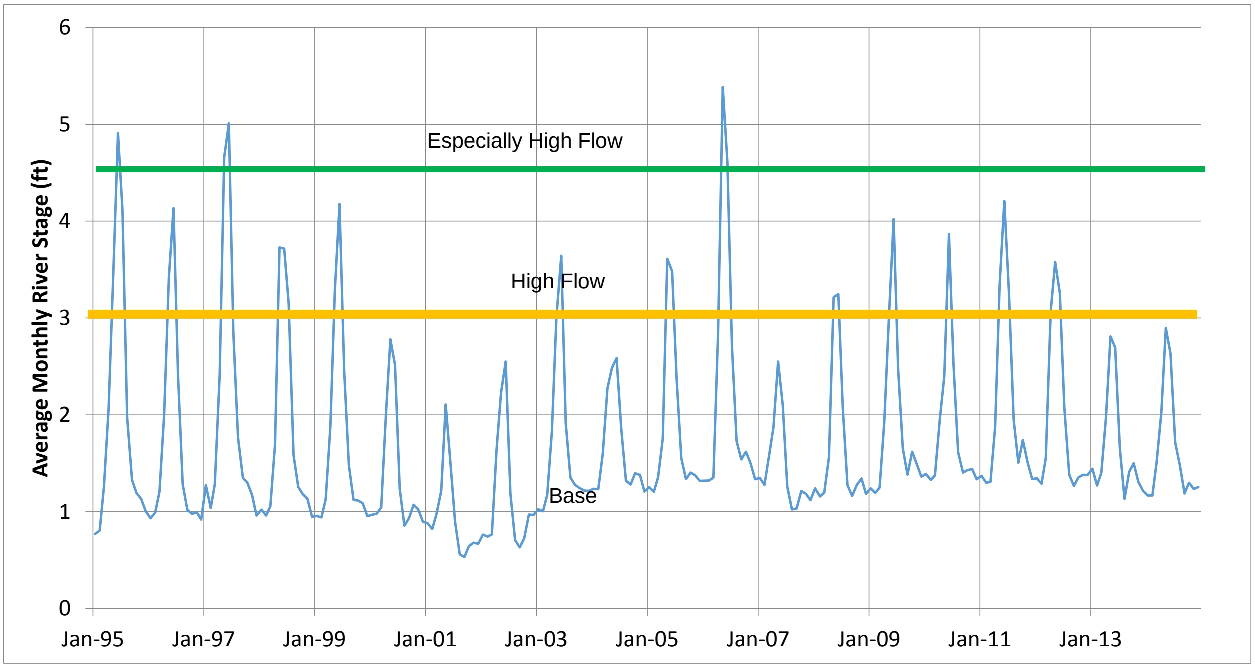

Figure 9. Average monthly stage recorded at Hailey.

Figure 10a shows the range of calibrated riverbed-conductance values for the Big Wood River with the base riverbed conductance for the Glendale Road to Sluder Road and Sluder Road to Wood River Ranch subreaches. Figures 10b and 10c show the riverbed conductance for higher flow conditions.

Figure 11 shows the range of calibrated riverbed-conductance values used to simulate aquifer and river interactions for Silver Creek and Willow Creek.

Figure 12a through 12d show the observed river gains and losses. Note that the gains depicted in Figure 12a frequently contain gaps during the spring. This is because of gage error at high flow and because there are several ungaged ephemeral tributary streams that likely contributed flow to the Big Wood River during this time; thus, not all the ungaged gains were contributions from the WRV aquifer system. The lack of tributary-stream measurements in these ephemeral streams and the possibility of gage error at high flows precludes calculation of reach gains and losses during these periods.

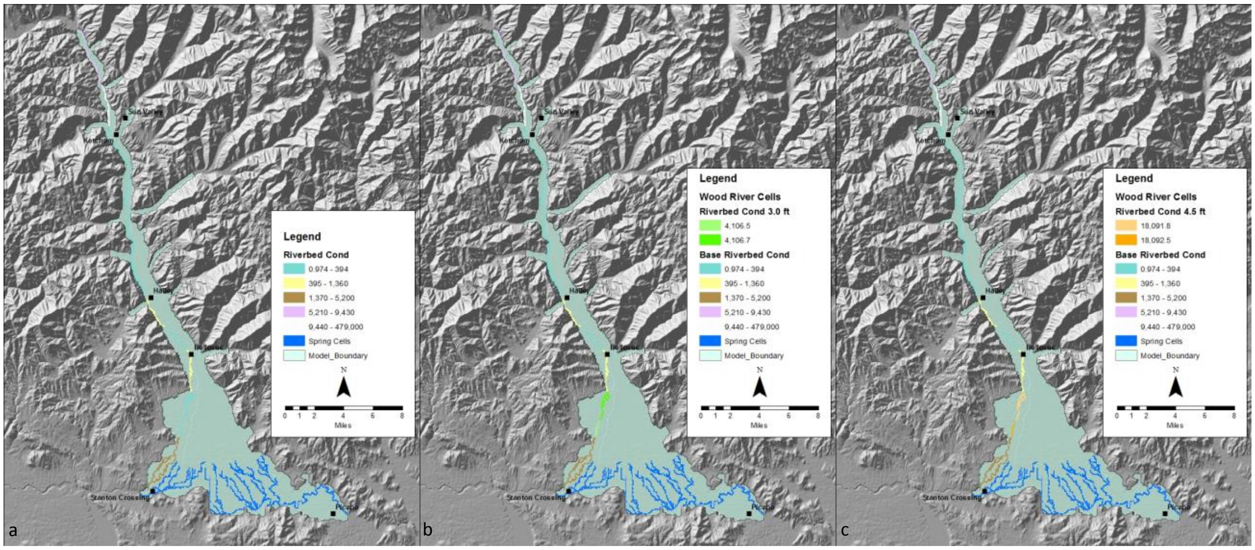

Figure 10. Calibrated riverbed conductance for the Big Wood River.

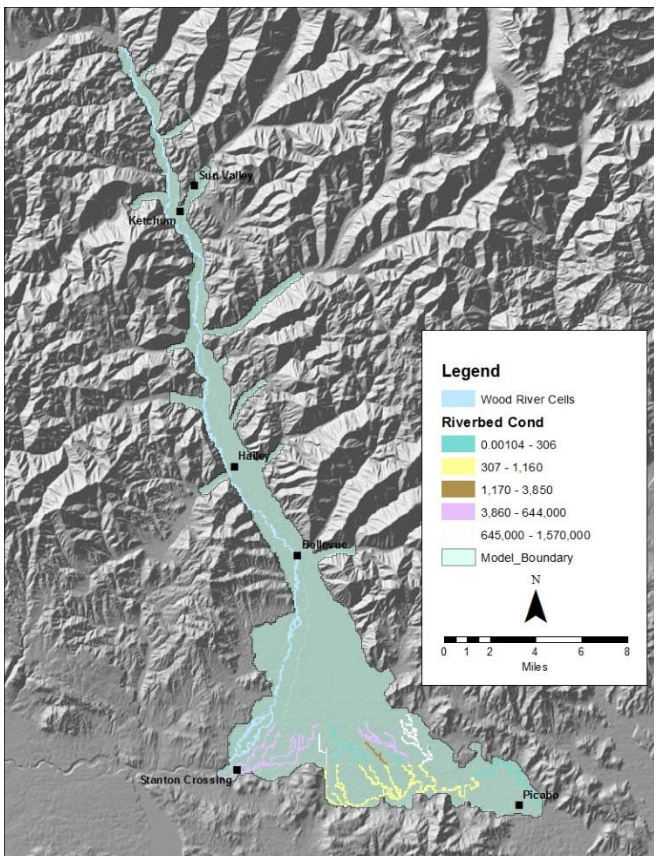

Figure 11. Calibrated riverbed conductance for Willow Creek and Silver Creek.

Head-dependent outlet boundaries

Groundwater leaves the WRV aquifer system as subsurface outflow at the Stanton Crossing and Silver Creek outlet boundaries (Figure 13). This was represented using drain cells in the WRV Aquifer Model Version 1.1. MODFLOW drain cells function much like MODFLOW river cells, except water can only flow from the aquifer out through the drain. No water can flow into the aquifer through the drain.

Drains were emplaced in each active model layer at both boundaries (one layer at the Stanton Crossing outlet boundary, three layers at the Silver Creek boundary). The table in Figure 13 shows the calibrated drain-conductance values. The average modeled discharge out the Stanton Crossing boundary is 275 AF (0.38 cfs); the average discharge out the Silver Creek boundary is 22,942 AF (31.7 cfs). Previous estimates of discharge beneath Stanton Crossing by other researches range from 0-300 AF and previous estimates of discharge beneath Silver Creek range from 4,000-53,000 AF (Fisher and others, 2013).

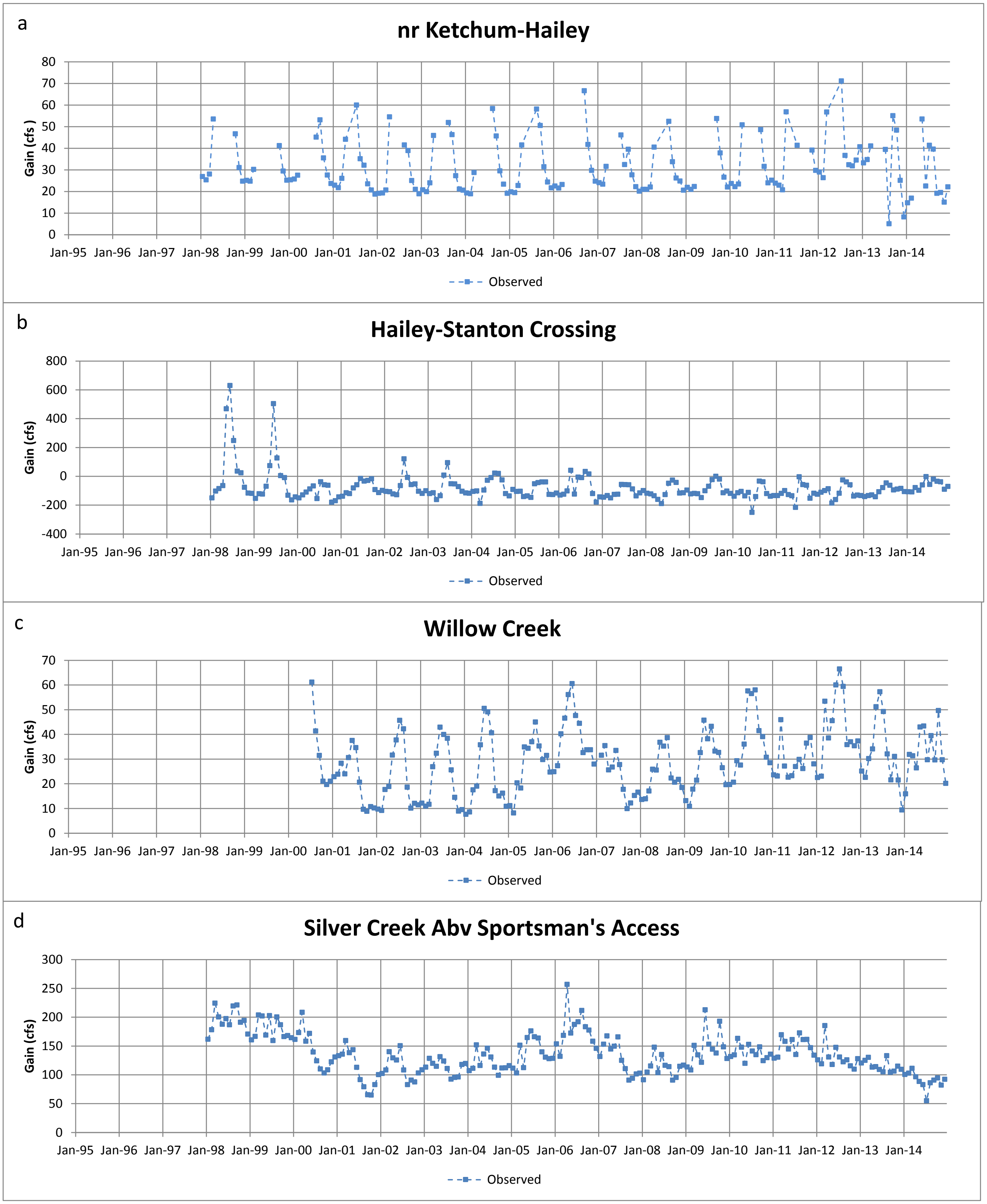

Figure 12. Observed river gains.

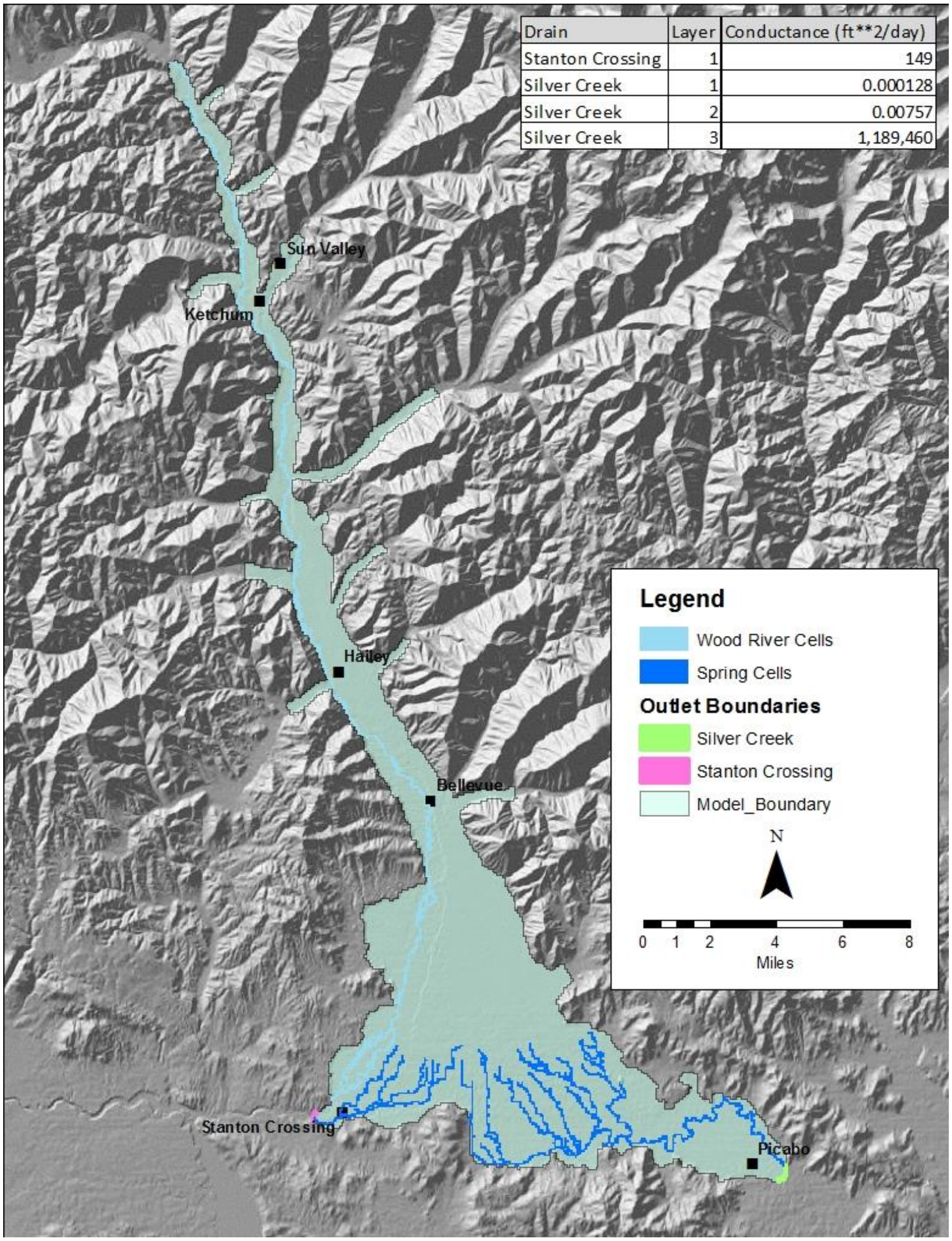

Figure 13. Model drain locations.

Assessment of Model Calibration

One of the measures of the quality of an aquifer model calibration is how closely the simulated data match with the field observations. This section describes the modeled and observed match for the various observation groups. When working with PEST, the residual, or the difference between the observed value and the modeled value is calculated by subtracting the modeled value from the observed value (Doherty, 2016); thus, a negative residual indicates that the modeled value is too high.

River gain and loss data

Figure 14a through 14d show simulated and observed gains for the Near Ketchum-Hailey, Hailey-Stanton Crossing, Willow Creek, and Silver Creek above Sportsman's Access reaches. Field data indicate that Silver Creek below Sportsman's Access gage has no interaction with the regional aquifer system (Wylie, 2019). Figure 8a shows the location of the reaches.

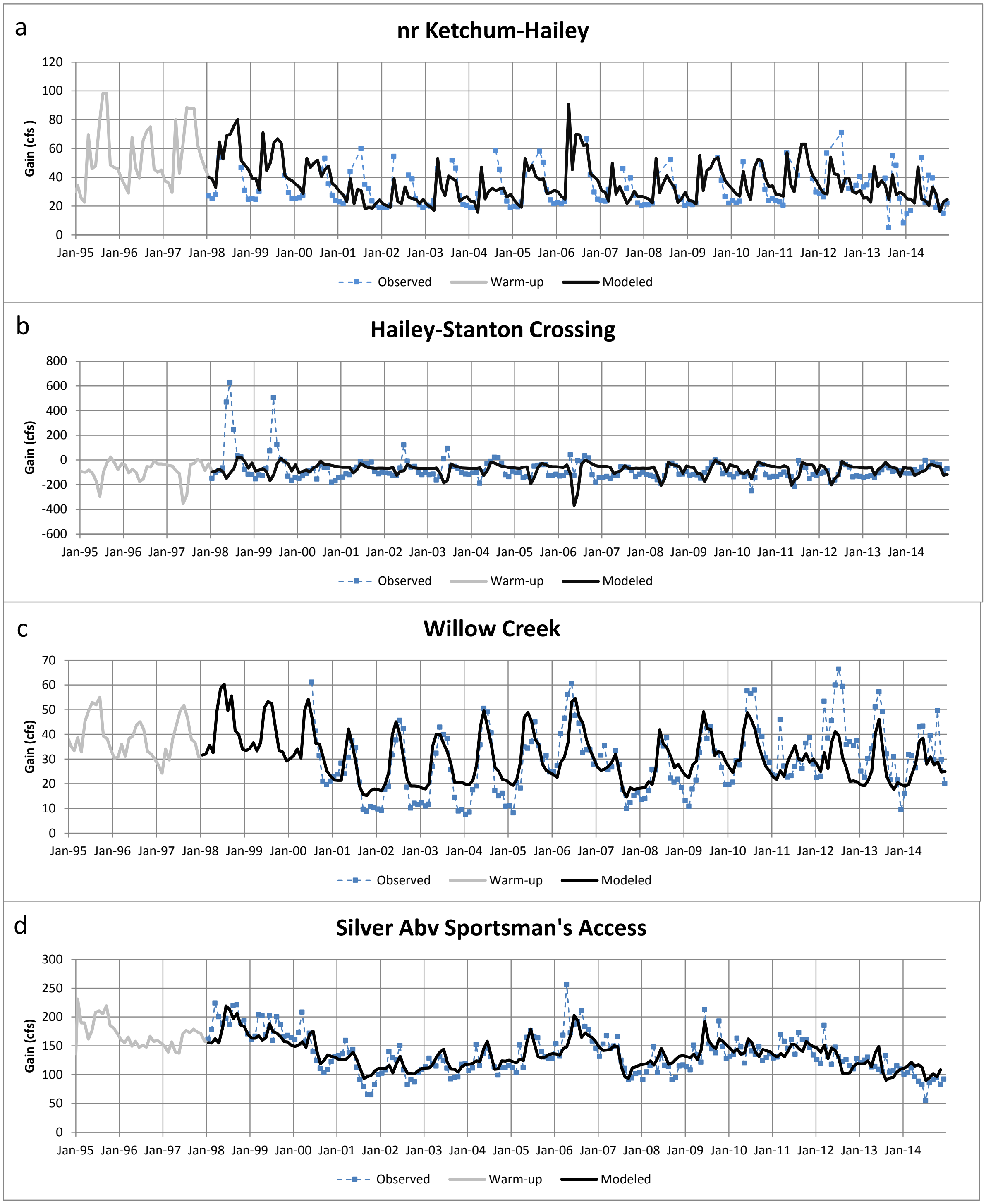

Figure 14. Modeled and observed river gains and losses.

Big Wood River

During the calibration period (1998-2014), the fall through early spring river-aquifer exchange in the near Ketchum-Hailey reach of the Big Wood River (Figure 8a) were calculated; however, because of gage error and ungaged tributary stream contributions, the spring and early summer aquifer and river interactions could not be determined. Figure 14a shows that the observed gains tend to be high in the spring, occasionally more than 60 cfs, and taper down to 20 cfs during the winter months. The WRV Aquifer Model Version 1.1 tends to capture the general character but misses the early season gains in some years. For example the WRV Aquifer Model Version 1.1 does not match the peak gains during the springs of 2001 and 2002.

Ungaged tributary stream contributions to the Hailey-Stanton Crossing reach (Figure 8a) during the late spring and summer are expected to be negligible, allowing calculation of year-round calibration targets. This reach tends to lose water to the aquifer; however, during the summers of 1998, 1999, 2002, 2003, 2004, and 2006 the field data show gains from the aquifer. The calculated gains may be the result of gage error during high flow. The modeled data match the seasonal highs and lows adequately; however, the field measurements tend to gradually decline throughout the summer and winter, while the modeled data drops abruptly. In reality, the Big Wood River gradually dries up between Glendale Road and Wood River Ranch, but in the model, the river either has water, or does not have water. Perhaps the inability to match the gradual decline is due to these abrupt changes in the model river file in the Glendale Road to Wood River Ranch subreach that are intended to simulate the change from high flow conditions during spring runoff to a dry riverbed at the end of summer.

Willow Creek

Willow Creek originates as springs within the model area and is gaged near the southwestern corner of the model (Figure 1). Figure 14c shows the field observations and the modeled match for Willow Creek. The modeled gains match the general shape of the field observations and match the timing of the peak discharge; however, the modeled data does not match the observed seasonal amplitude. The observed data almost certainly contain some runoff from spring snowmelt, which is not represented in the model.

Silver Creek

Silver Creek originates as springs within the model area and is measured at the Sportsman's Access gage shown in Figure 1. Figure 14d shows the field observations and the modeled match. The modeled gains follow the general shape of the field observations but under-predict the seasonal amplitude. Perhaps the mismatch is because peak flows contain some runoff from spring snowmelt.

Several streamflow measurements collected in Silver Creek just north of Picabo suggest that there is minimal aquifer-river interaction between Silver Creek and the WRV aquifer downstream (east) of the Sportsman's Access gage (Wylie, 2019). This finding is consistent with historic seepage studies (Moreland, 1977).

Seepage surveys

Improved resolution of the aquifer-river interaction along the Big Wood River and Silver Creek is possible through incorporating the results of the August 2012, October 2012, and March 2013 seepage surveys (Bartolino, 2014). The modeled match with the three seepage surveys is shown in Figure 15. One of the challenges associated with including the seepage surveys is that the field results are point measurements influenced by daily or even hourly water-management decisions, while the model is responding to average monthly water use. Even so, the cross plot in Figure 15 shows that the model output matches reasonably well. If the model output were to match the field observations perfectly, the data would fall on the 45° line. The fact that the data do not all fall on the 45° line may be, in part, because the diversions and returns fluctuated from the average during the seepage survey.

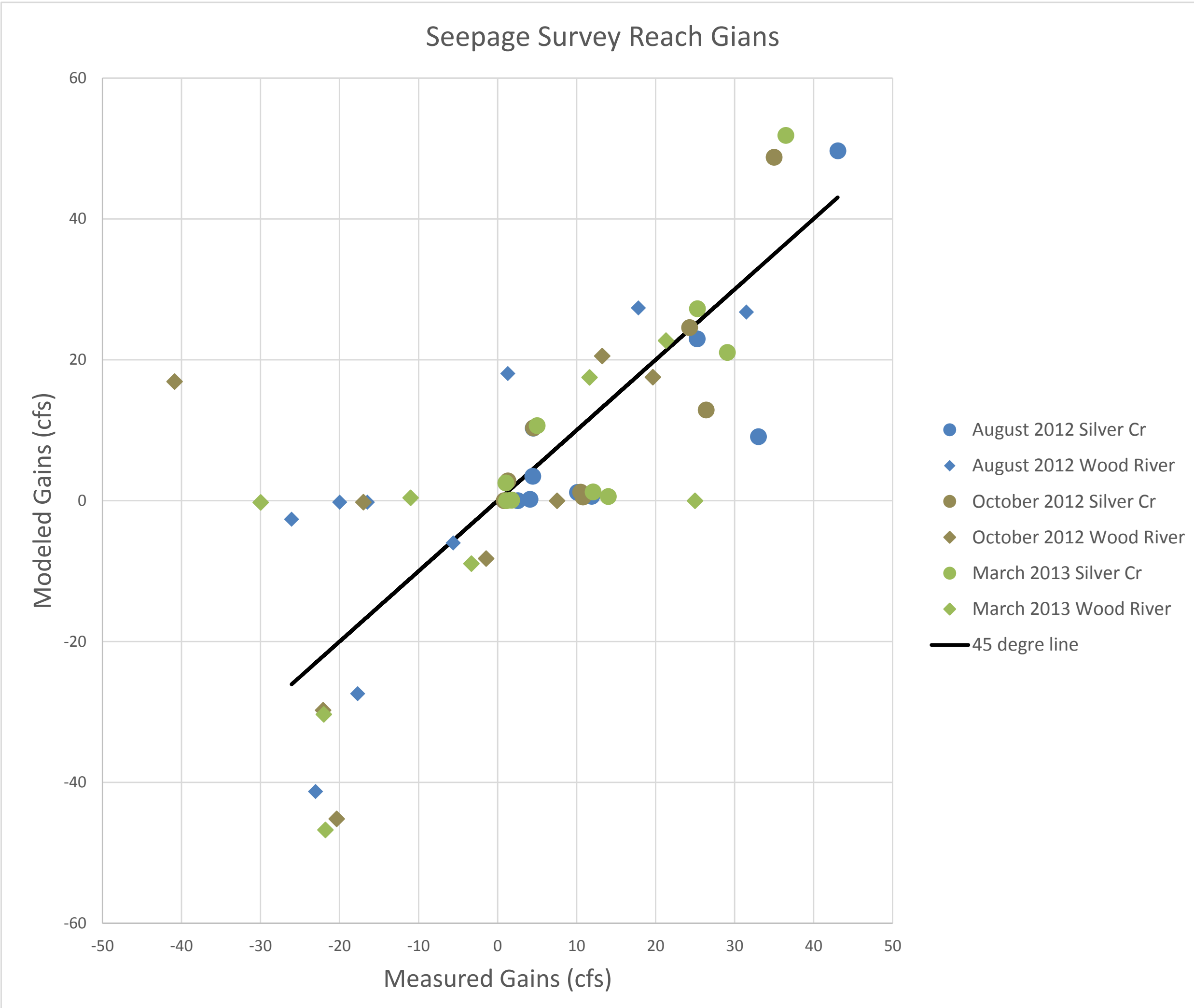

Figure 15. Cross plot of modeled and observed seepage survey reach gains.

Heart Rock Ranch-Stanton Crossing gains

When the flow downstream of the Heart Rock Ranch point of diversion on the Big Wood River is zero, the flow measured at the Stanton Crossing gage represents the gains accrued between the Heart Rock Ranch point of diversion and the Stanton Crossing gage (Figure 16). This situation happened 89 times during the simulation period, and the chart in Figure 16 shows the field observations compared with the modeled values. Some of the mismatch is due to the fact that the seasonal changes to the modeled river are more granular than in the actual river. The Big Wood River between Wood River Ranch and Stanton Crossing is modeled as containing water when Landsat images show water in more than half the reach. The real world situation is much more complex and the wetted length of the river can change daily. This likely explains the deviation between modeled and measured data in the winter of 2007-2008.

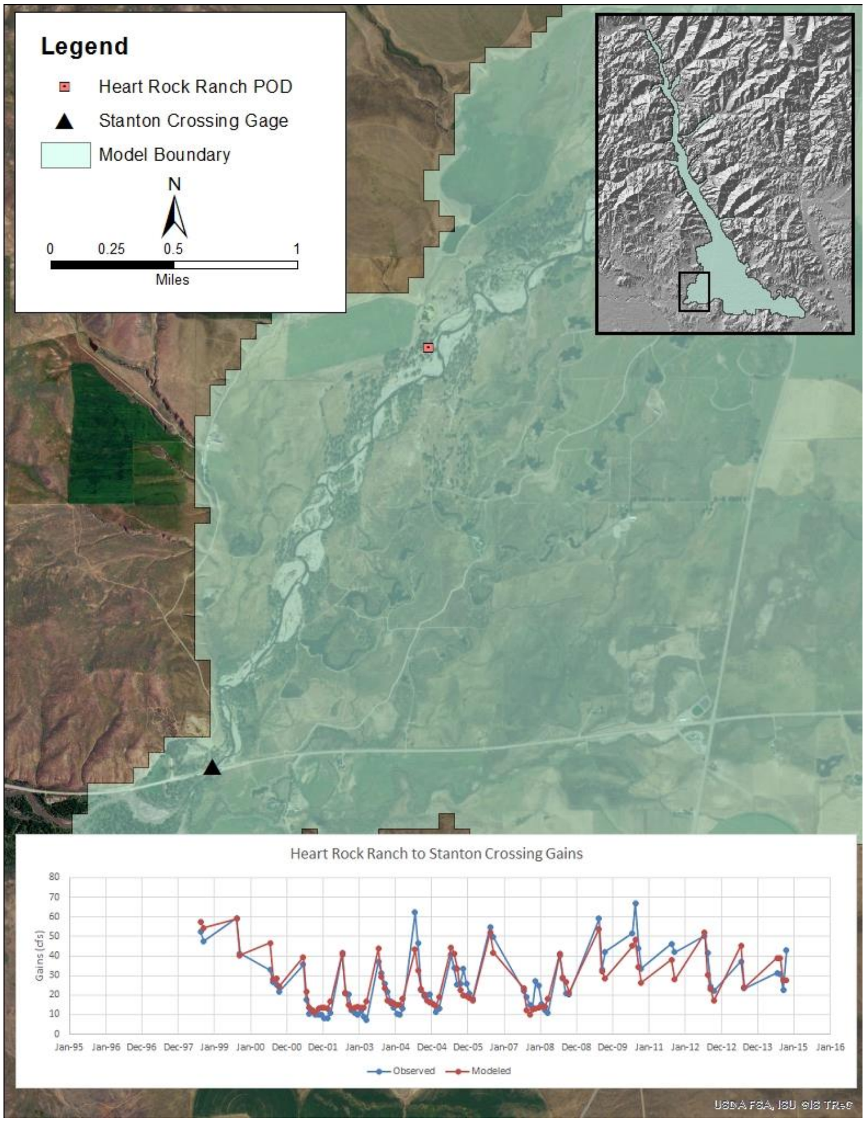

Figure 16. Heart Rock Ranch to Stanton Crossing gains.

Aquifer head in observation wells

One thousand one hundred one water levels collected in the 129 wells shown in Figure 17 were used as calibration data. The wells were surveyed using a real-time kinematic and fast-static differential global positioning surveying system capable of sub-foot elevation accuracy. Water levels were collected using an electric measuring tape, a steel tape, a pressure gage, or a pressure transducer. The resulting water-level elevations are considered accurate to ±1.0 ft.

This carefully documented water-level dataset provides excellent calibration data. The water level calibration statistics are presented in the table in Figure 17. The mean difference between modeled and observed water levels is -0.15 feet, the median difference is 0.18 feet, and the standard deviation is 5.92 feet. The 95% confidence interval for the mean is ± 0.35 feet; thus the confidence interval extends from +0.20 to -0.50 and includes zero. Therefore the possibility that the mean residual is zero cannot be excluded.

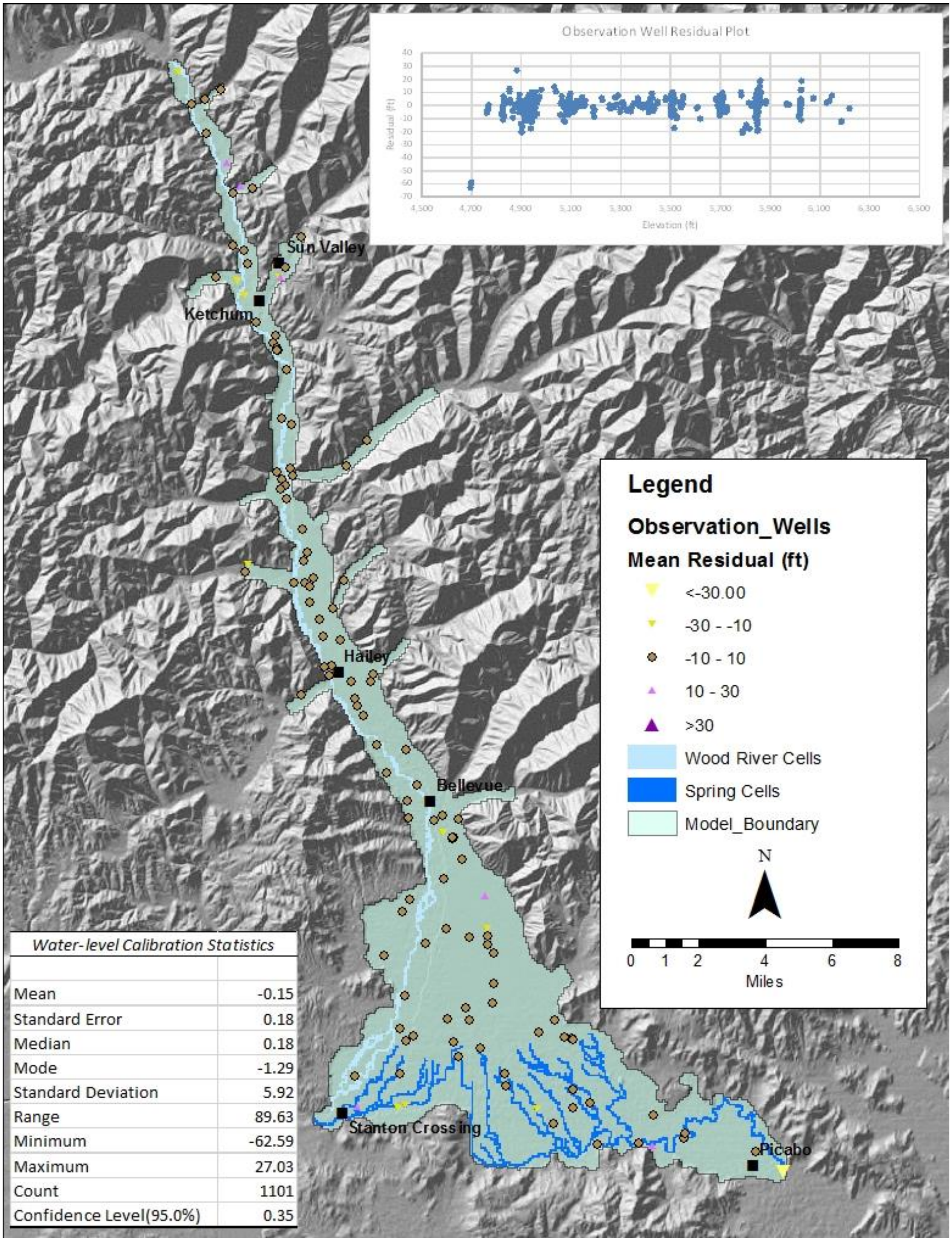

Water-level Calibration Statistics	
Mean	-0.15
Standard Error	0.18
Median	0.18
Mode	-1.29
Standard Deviation	5.92
Range	89.63
Minimum	-62.59
Maximum	27.03
Count	1101
Confidence Level(95.0%)	0.35

Figure 17. Residual plot and calibration statistics for observation well data.

The residual-plot in Figure 17 is a graph of the difference between observed and modeled water levels plotted with the observed elevation on the X axis. Assuming a perfect match between measured and modeled water levels, the blue circles representing individual water level observations would all fall on the zero line. There are two significant deviations from the zero line, one at the elevation of 4,700 feet, which correlates to the yellow downward-pointing triangle east of Picabo in Figure 17. There are four observations in this well and the model is unable match them and match the observations in the well just north of Picabo with 19 observations. The other deviation shown in the residual-plot in Figure 17 is near the elevation of 4,900 feet. It corresponds to the purple upward pointing triangle near Stanton Crossing. The well is modeled as being completed in the unconfined aquifer and perhaps, in reality, it was completed in the confined aquifer.

Figure 18a through 18c show hydrographs of modeled water levels with observed water levels for three wells. Hydrographs showing the modeled match with field observations for all wells with more than four field measurements are included in Appendix A.

Geolocated well driller water-levels

The Geolocated wells were all measured by a well driller after completing a well. The well locations were determined by either a hand-held GPS measurement provided by the driller, or an address for the lot on which the well was drilled (Figure 19). The land-surface elevation was determined from a digital elevation model. The method for obtaining the water level is unknown. The assumed accuracy for the Geolocated wells is ±7.0 ft. These water-levels were not collected with the documented accuracy of the Observation wells and none of the wells have repeated measurements. However, this dataset is useful because, as Figure 20 shows, it provides measurements during a time when the Observation well dataset is sparse. The mean difference between modeled and measured values is -4.00 feet, the median is -0.74 feet, and the standard deviation is 29.02 ft. The 95% confidence interval for the mean is ±3.92 feet; thus the 95% confidence interval extends from -0.08 to -7.92 ft.

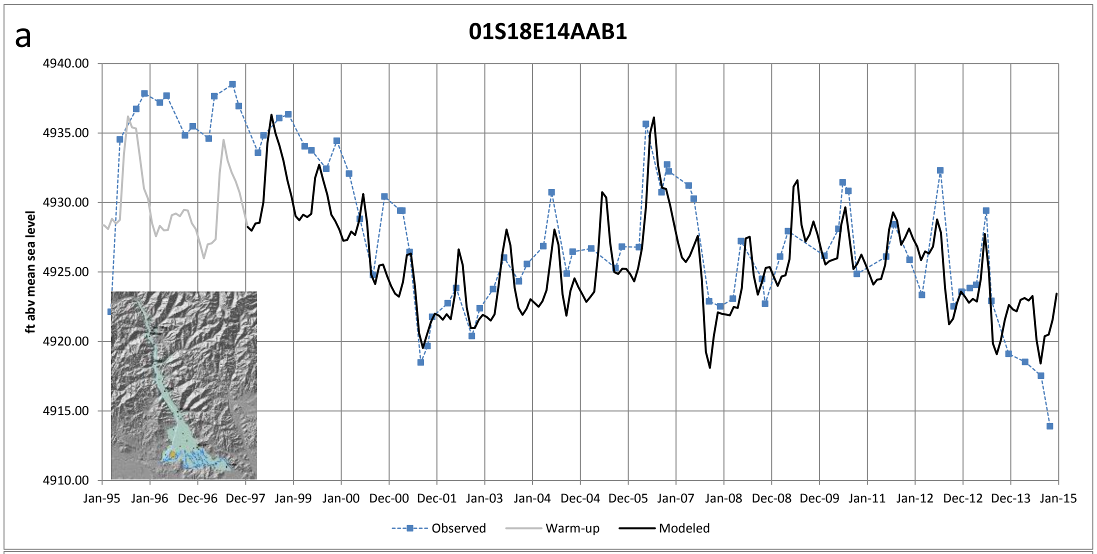

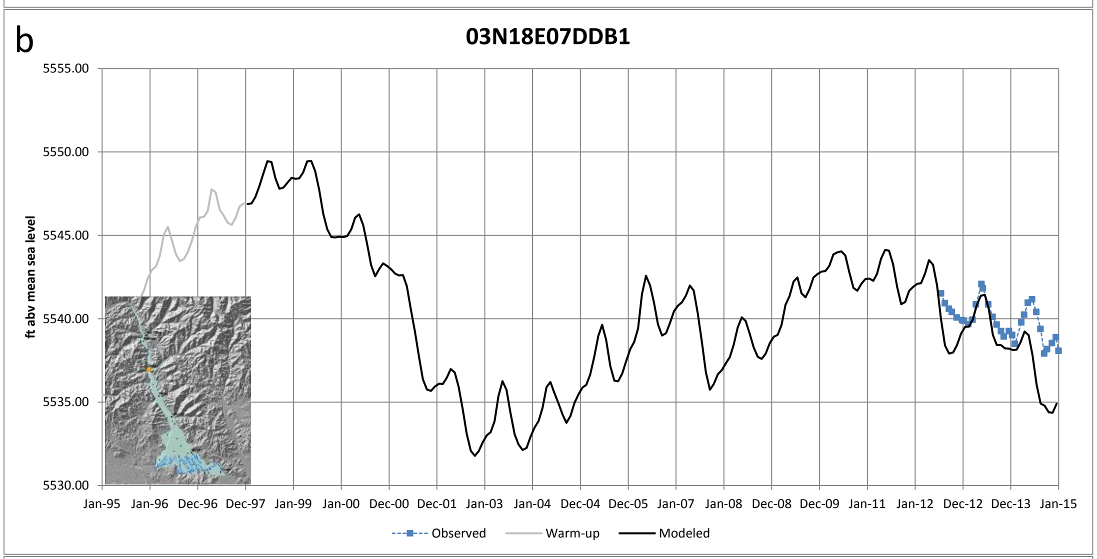

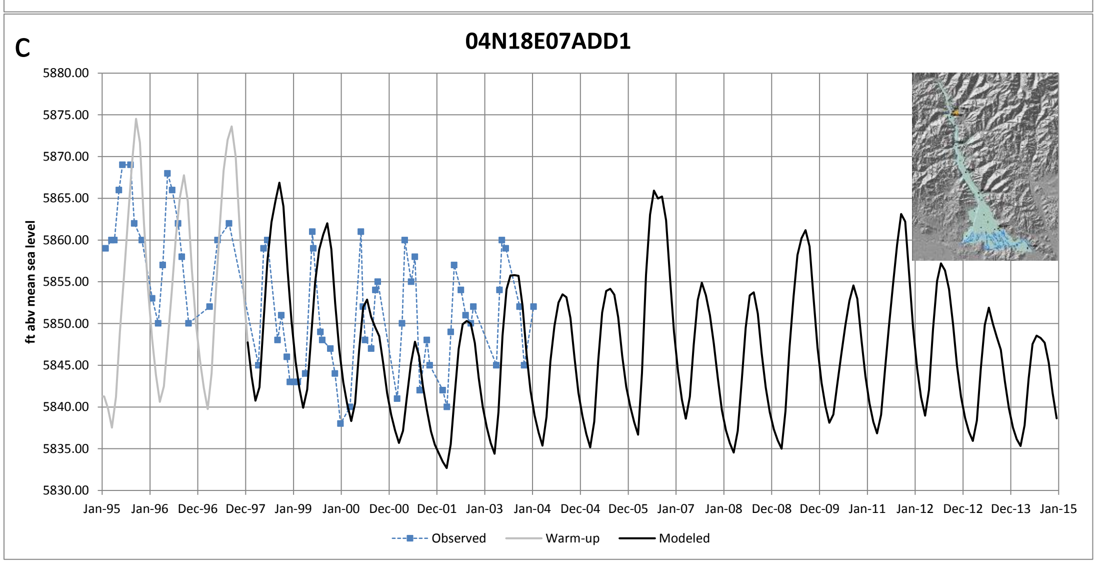

Figure 18. Match between modeled and observed water levels.

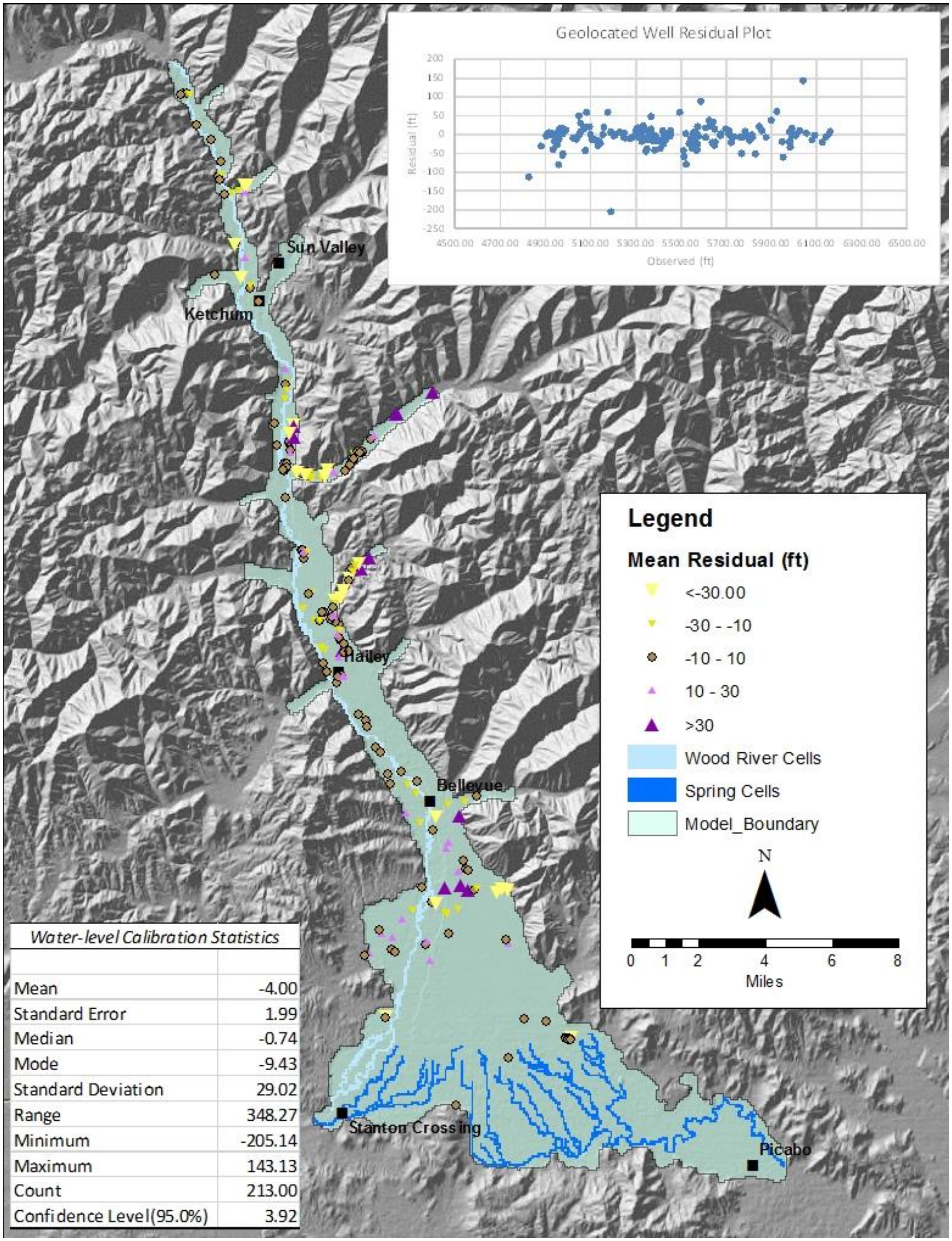

Mean	-4.00
Standard Error	1.99
Median	-0.74
Mode	-9.43
Standard Deviation	29.02
Range	348.27
Minimum	-205.14
Maximum	143.13
Count	213.00
Confidence Level(95.0%)	3.92

Figure 19. Residual plot and calibration statistics for geolocated well data.

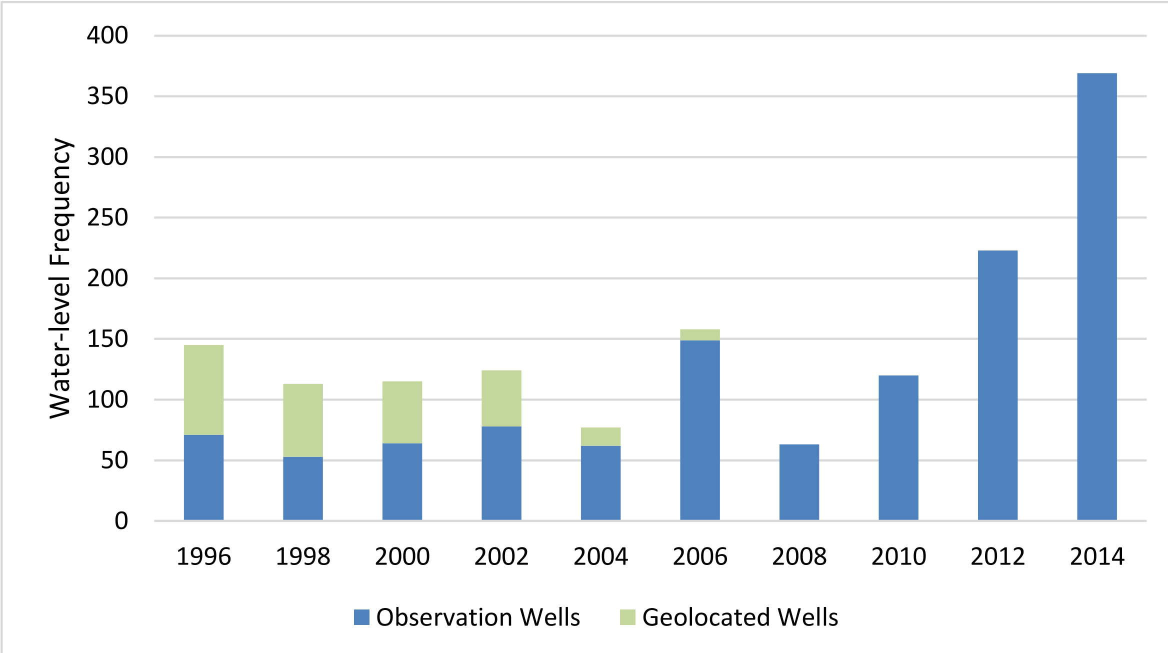

Figure 20. Frequency of water level observations through time.

Conclusions

This report documents the recalibration of the WRV Aquifer Model. WRV Aquifer Model Version 1.1 was calibrated to 16 years of data (1998-2014) as compared to 12 years for WRV Aquifer Model Version 1.0 (1998-2010). The Version 1.1 calibration period includes some of the driest years on record (2001, 2004 and 2007) and some of the wettest years on record (1996 and 2006). Calibration to data from a wide range of hydrologic conditions increases the likelihood that the model will accurately simulate the response of the river and aquifer system to a broad range of stresses.

The goal of this recalibration was to develop a more robust representation of the basin hydrogeology. Some of the improvements include an improved representation of the areal and temporal extent of reaches within the Big Wood River that seasonally go dry. Improved calibration data include a mass measurement conducted in 2012, 18 wells with pressure transducers, and the inclusion of the Heart Rock Ranch to Stanton Crossing reach-gain target.

Despite these enhancements our understanding of the WRV Aquifer System remains imperfect and more work needs to be done. Several significant gaps in data or in the understanding of the underlying hydrologic system have become apparent during this project. Suggestions for future work include:

a) Install transducers in as many tributary valley wells as possible,

b) Monitor several of the ephemeral streams in the tributary valleys above Hailey to determine the duration of spring runoff,

c) Monitor and archive recharge events within the WRV,

d) Continue annual fall seepage studies on Trail Creek and Warm Springs Creek,

e) Continue stream gaging at the Big Wood River near Ketchum, Big Wood River at Hailey, Big Wood River at South Broadford Bridge, Big Wood River at Stanton Crossing, North Fork Big Wood River near Sawtooth National Recreation Area, Trail Creek Near Sun Valley, Trail Creek at Ketchum, Warm Springs Creek at Gates Road, Warm Springs Creek near Ketchum, East Fork Big Wood River at Gimlet, Willow Creek near Spring Creek Ranch, and Silver Creek at Sportsman Access,
f) Continue Big Wood River stage measurements at Hulen Road Bridge, at Ketchum, at Gimlet, at Glendale Bridge, and at Wood River Ranch,
g) Continue monitoring a minimum of 45 observation wells in the WRV, and
h) Continue annual (at a minimum) gaging of Silver Creek at the North Picabo Road Bridge.

Although every groundwater model is a simplification of a complex hydrologic system, WRV Aquifer Model Version 1.1 is the best available tool for evaluating the interaction between groundwater and surface water in the Wood River Valley. The science underlying the production and calibration of the WRV Aquifer Model Version 1.1 reflects the best knowledge of the aquifer system available at this time. The WRV Aquifer Model Version 1.1 was calibrated to 1,314 aquifer water-level measurements and 1,026 river gain-and loss-calculations. Calibration statistics indicate a good fit to the observed data, providing confidence that the updated model provides an acceptable representation of the hydrologic system in the Wood River Valley.

With the Eastern Snake Plain Aquifer Model, the length of the Snake River in hydraulic communication with the Eastern Snake Plain Aquifer remains nearly constant through time allowing the development of a numerical superposition version of that model. However, in the WRV, the length of the Big Wood River in hydrologic connection with the aquifer system varies seasonally, thus a numerical superposition model based on the WRV Aquifer Model should not be developed (Hubbel and others, 1997). All analyses with the WRV Aquifer Model should be conducted using a fully populated transient model.

References

Allen, R., Robison, C.W., Garcia, M., Trezza, R., Tasumi, M., and Kjaersgaard, J., 2010, ETrF vs NDVI Relationships for Southern Idaho for Rapid Estimation of Evapotranspiration. Report to IDWR. University of Idaho, Kimberly, ID.

Allen, R., Tasumi, M., Trezza, R., and Kjaersgaard, J., 2010, METRIC Mapping Evapotranspiration at High Resolution Applications Manual for Landsat Satellite Imagery Version 2.07. University of Idaho, Kimberly, ID.

Allen, R.G., Pereira, L.S., Raes, D., and Smith, M., 1998, Crop evapotranspiration: Guidelines for computing crop water requirements: Rome, United Nations Food and Agriculture Organization, FAO Irrigation and Drainage Paper 56.

Bartolino, J.R., 2014, Stream seepage and groundwater levels, Wood River Valley, south-central Idaho, 2012–13: U.S. Geological Survey Scientific Investigations Report 2014-5151.

Doherty, J.E., 2003, Ground Water Model Calibration Using Pilot Points and Regularization, Ground Water. 41, no. 2: 170-177.

Doherty, J.E., 2016, PEST, Model-Independent Parameter Estimation-User Manual, 6th ed. Watermark Numerical Computing.

Fisher, J.C., Bartolino, J.R., Wylie, A.H., Sukow, J., and McVay, M., 2016, Groundwater-flow model of the Wood River Valley aquifer system, south-central Idaho: U.S. Geological Survey Scientific Investigations Report 2016-5080.

Freeze, R.A., J.A. Cherry, 1979, Groundwater. Prentice-Hall.

Hubbel, J.M., Bishop, C.W., Johnson, G.S., Lucas, J.G., 1997, Numerical Ground-Water Flow Modeling of the Snake River Plain Aquifer Using the Superposition Technique, Ground Water. 35, no. 1: 59-66.

McVay, M., 2014, Draft Design Document: Calculating Evapotranspiration during the Growing Season.

Moreland, J.A., 1977, Ground water-surface water relations in the Silver Creek area, Blaine County, Idaho: U.S. Geological Survey Open-File Report 77-456

Panday, Sorab, Langevin, C.D., Niswonger, R.G., Ibaraki, Motomu, and Hughes, J.D., 2013, MODFLOW-USG Version 1: An unstructured grid version of MODFLOW for simulating groundwater flow and tightly coupled process using and control volume finite-difference formulation, in U.S. Geological Survey Techniques and Methods 6-A45.

Sanders, L.L., 1998, A Manual of Field Hydrogeology. Prentice-Hall.

Sukow, J., 2014, Draft Design Document: Reach Gain Calibration Targets for the Big Wood River and Silver Creek.

Wylie, A.H., 2019, Seven Silver Creek Flow Measurements Collected at North Picabo Road Bridge between October 2014 and November 2018.

Appendix A

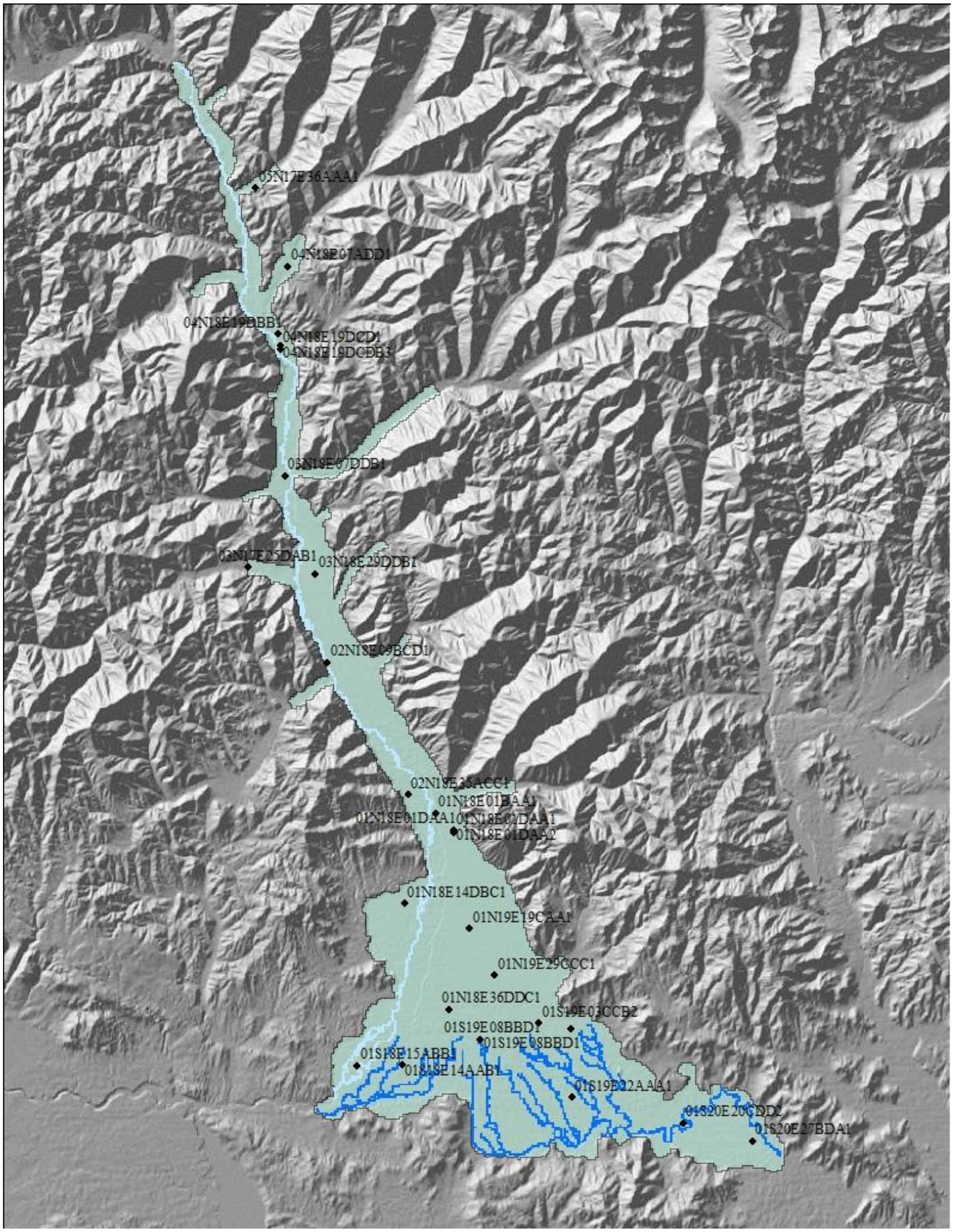

Figure 21. Locations of wells with more than four observations.

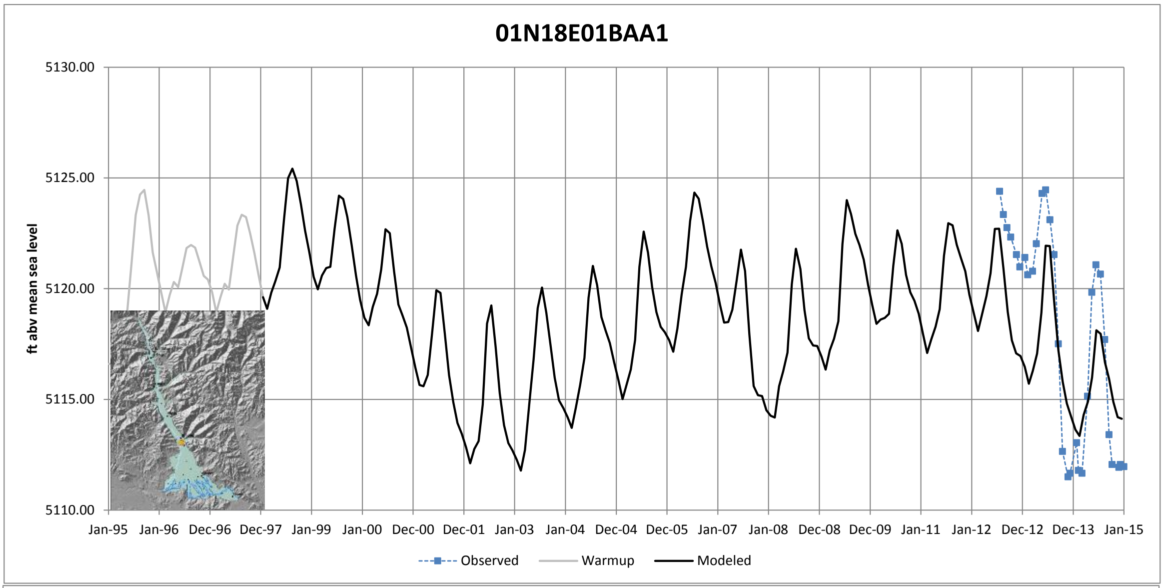
01N18E01BAA1
5130.00
5125.00
5120.00
5115.00
5110.00
ft abv mean sea level
Jan-95 Jan-96 Dec-96 Dec-97 Jan-99 Jan-00 Dec-00 Dec-01 Jan-03 Jan-04 Dec-04 Dec-05 Jan-07 Jan-08 Dec-08 Dec-09 Jan-11 Jan-12 Dec-12 Dec-13 Jan-15
Observed
Warmup
Modeled

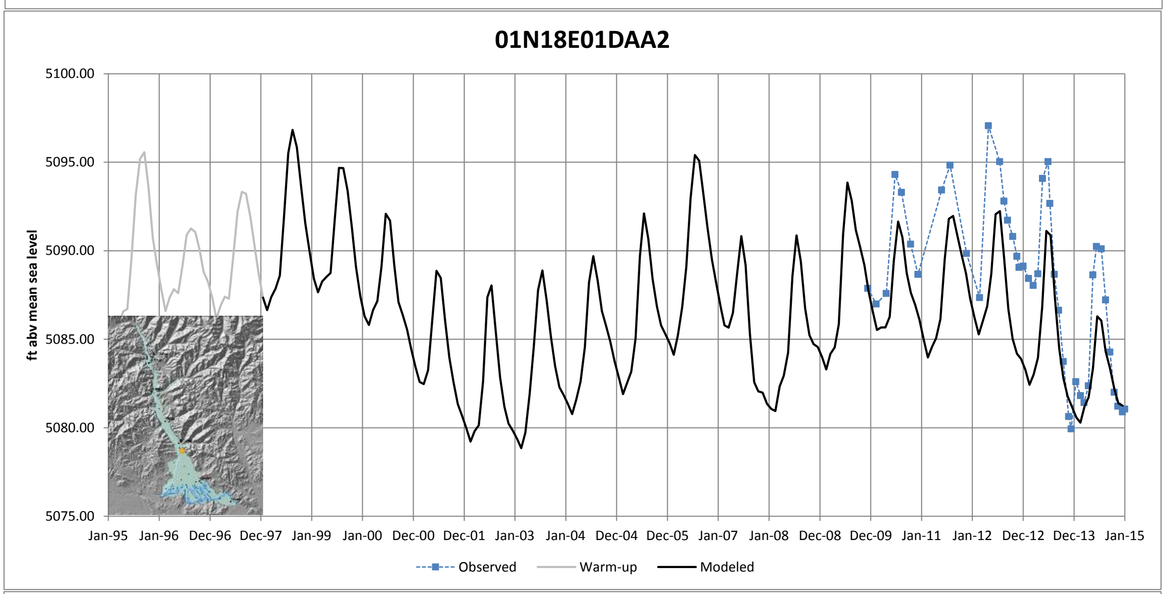
01N18E01DAA2
5100.00
5095.00
5090.00
5085.00
5080.00
5075.00
ft abv mean sea level
Jan-95 Jan-96 Dec-96 Dec-97 Jan-99 Jan-00 Dec-00 Dec-01 Jan-03 Jan-04 Dec-04 Dec-05 Jan-07 Jan-08 Dec-08 Dec-09 Jan-11 Jan-12 Dec-12 Dec-13 Jan-15
Observed
Warm-up
Modeled

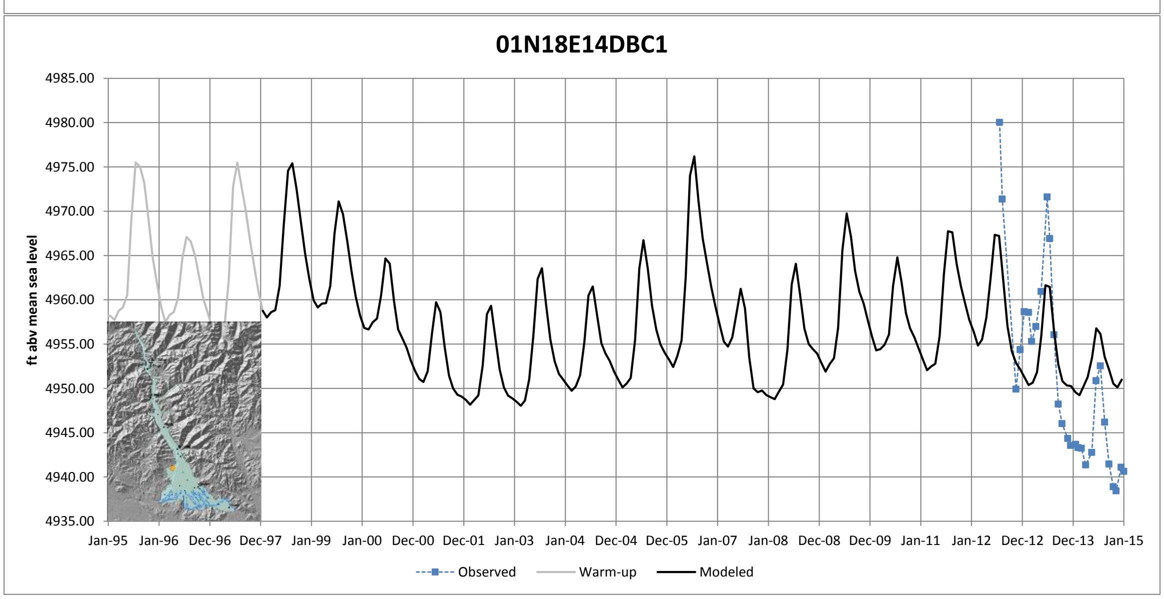
01N18E14DBC1
4985.00
4980.00
4975.00
4970.00
4965.00
4960.00
4955.00
4950.00
4945.00
4940.00
4935.00
ft abv mean sea level
Jan-95 Jan-96 Dec-96 Dec-97 Jan-99 Jan-00 Dec-00 Dec-01 Jan-03 Jan-04 Dec-04 Dec-05 Jan-07 Jan-08 Dec-08 Dec-09 Jan-11 Jan-12 Dec-12 Dec-13 Jan-15
Observed
Warm-up
Modeled

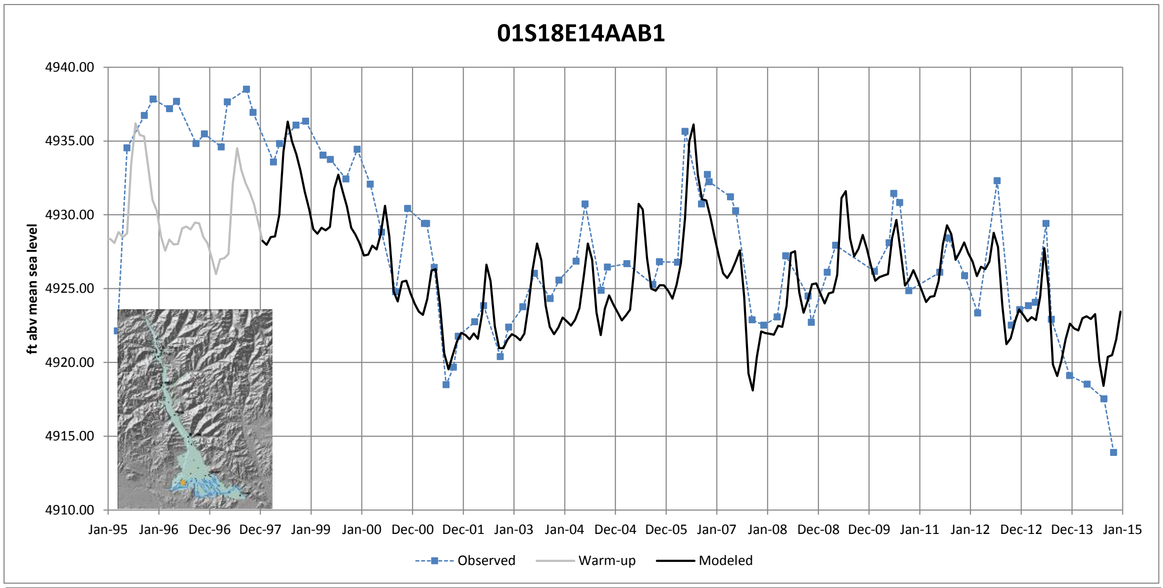
01S18E14AAB1
4940.00
4935.00
4930.00
4925.00
4920.00
4915.00
4910.00
ft abv mean sea level
Jan-95 Jan-96 Dec-96 Dec-97 Jan-99 Jan-00 Dec-00 Dec-01 Jan-03 Jan-04 Dec-04 Dec-05 Jan-07 Jan-08 Dec-08 Dec-09 Jan-11 Jan-12 Dec-12 Dec-13 Jan-15
Observed
Warm-up
Modeled

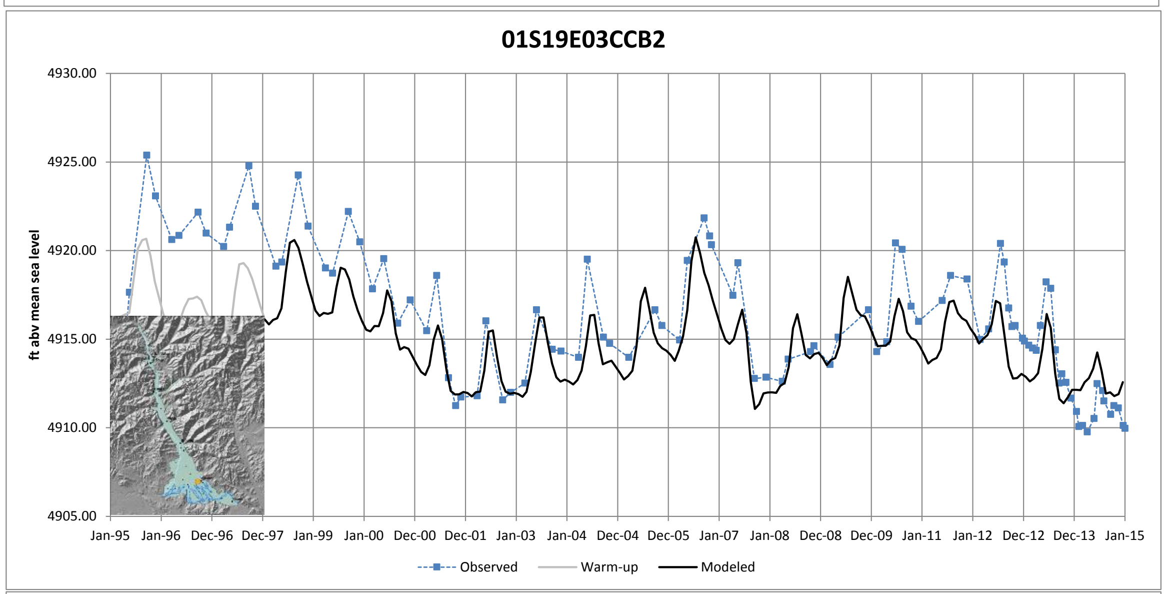
01S19E03CCB2
4930.00
4925.00
4920.00
4915.00
4910.00
4905.00
ft abv mean sea level
Jan-95 Jan-96 Dec-96 Dec-97 Jan-99 Jan-00 Dec-00 Dec-01 Jan-03 Jan-04 Dec-04 Dec-05 Jan-07 Jan-08 Dec-08 Dec-09 Jan-11 Jan-12 Dec-12 Dec-13 Jan-15
Observed
Warm-up
Modeled

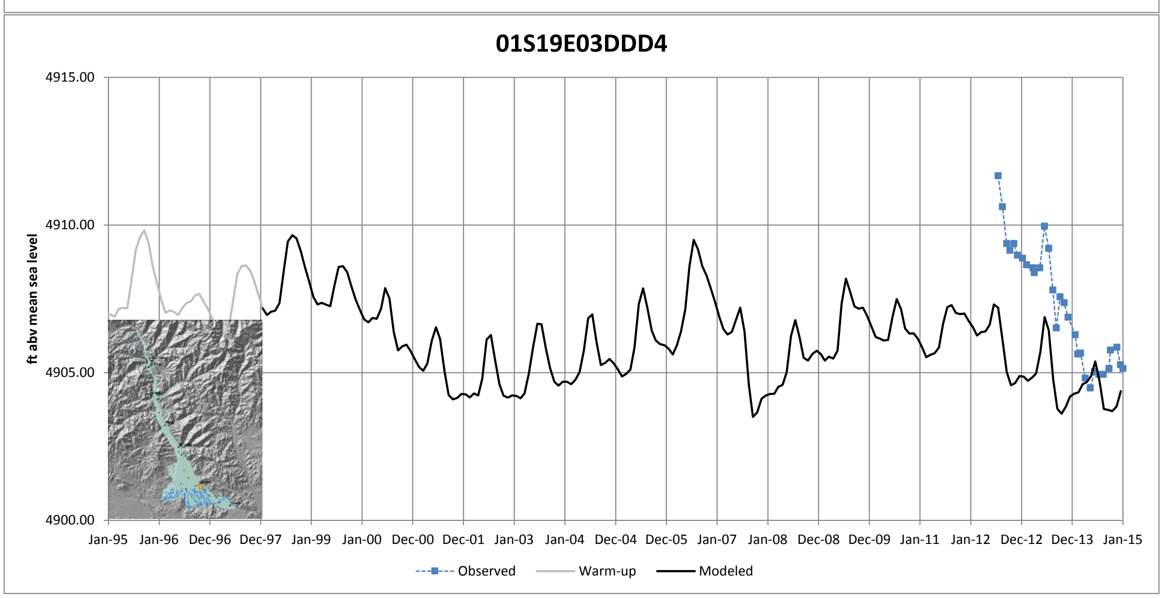
01S19E03DDD4
4915.00
4910.00
4905.00
4900.00
ft abv mean sea level
Jan-95 Jan-96 Dec-96 Dec-97 Jan-99 Jan-00 Dec-00 Dec-01 Jan-03 Jan-04 Dec-04 Dec-05 Jan-07 Jan-08 Dec-08 Dec-09 Jan-11 Jan-12 Dec-12 Dec-13 Jan-15
Observed
Warm-up
Modeled

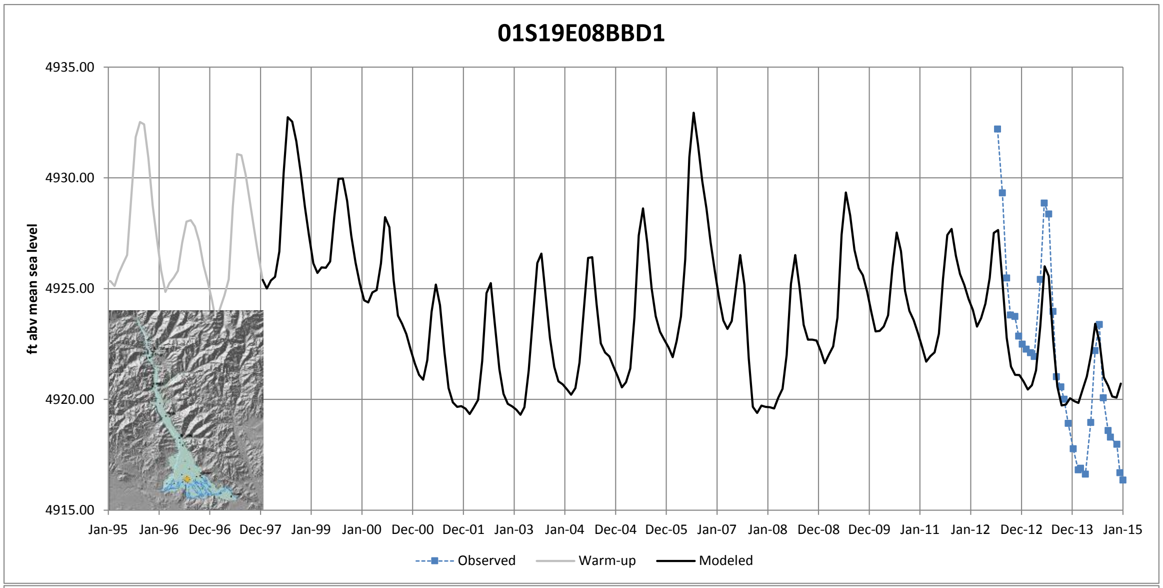
01S19E08BBD1
ft abv mean sea level
4935.00
4930.00
4925.00
4920.00
4915.00
Jan-95
Jan-96
Dec-96
Dec-97
Jan-99
Jan-00
Dec-00
Dec-01
Jan-03
Jan-04
Dec-04
Dec-05
Jan-07
Jan-08
Dec-08
Dec-09
Jan-11
Jan-12
Dec-12
Dec-13
Jan-15
Observed
Warm-up
Modeled

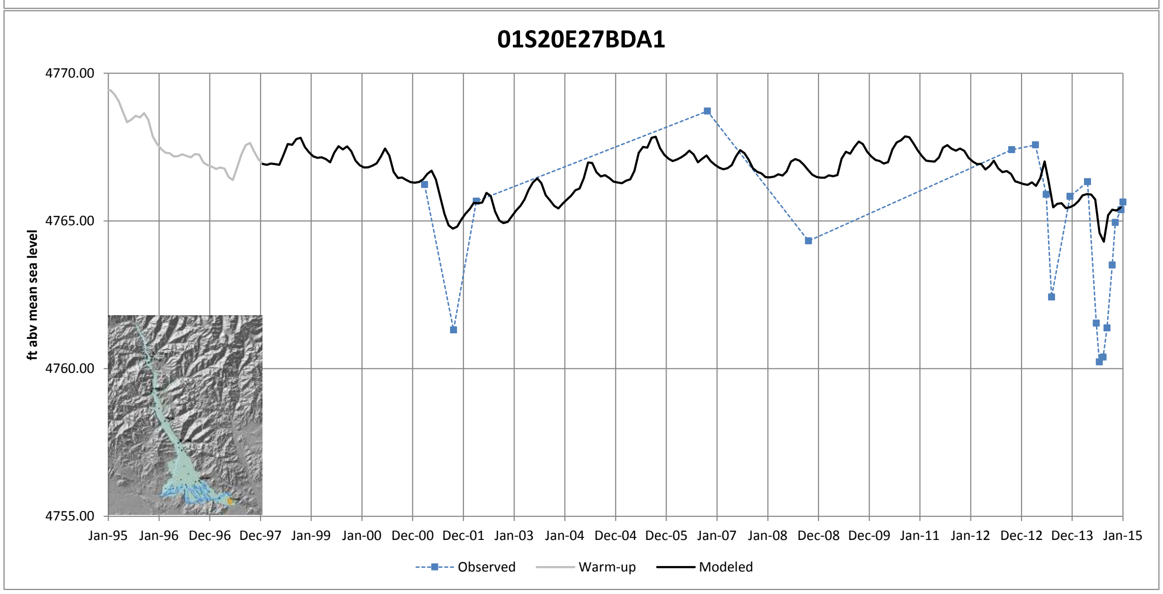
01S20E27BDA1
ft abv mean sea level
4770.00
4765.00
4760.00
4755.00
Jan-95
Jan-96
Dec-96
Dec-97
Jan-99
Jan-00
Dec-00
Dec-01
Jan-03
Jan-04
Dec-04
Dec-05
Jan-07
Jan-08
Dec-08
Dec-09
Jan-11
Jan-12
Dec-12
Dec-13
Jan-15
Observed
Warm-up
Modeled

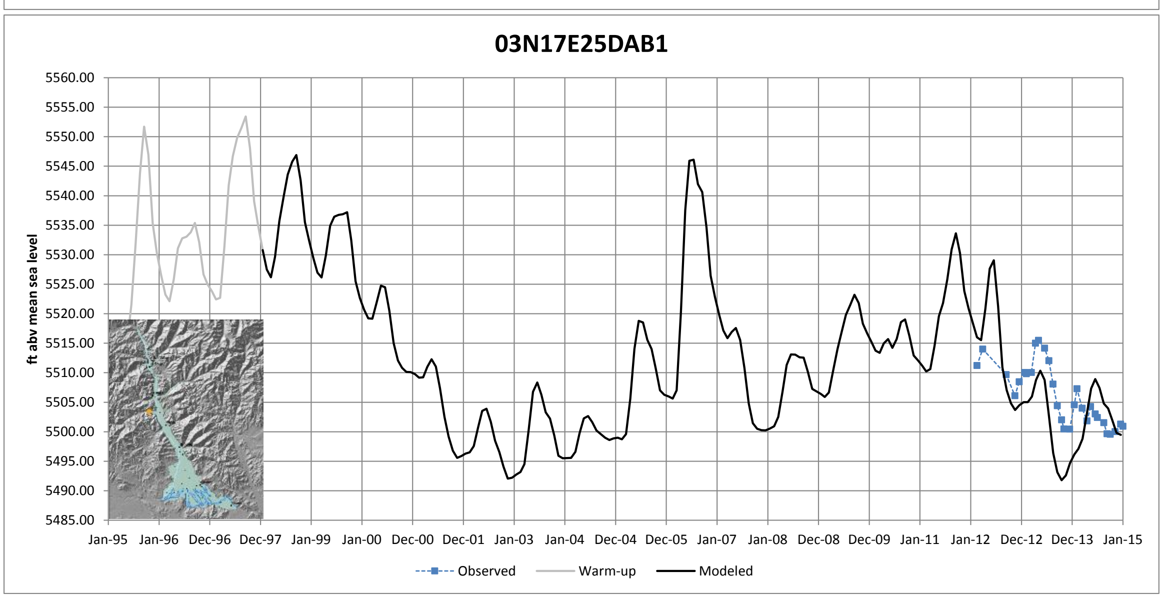
03N17E25DAB1
ft abv mean sea level
5560.00
5555.00
5550.00
5545.00
5540.00
5535.00
5530.00
5525.00
5520.00
5515.00
5510.00
5505.00
5500.00
5495.00
5490.00
5485.00
Jan-95
Jan-96
Dec-96
Dec-97
Jan-99
Jan-00
Dec-00
Dec-01
Jan-03
Jan-04
Dec-04
Dec-05
Jan-07
Jan-08
Dec-08
Dec-09
Jan-11
Jan-12
Dec-12
Dec-13
Jan-15
Observed
Warm-up
Modeled

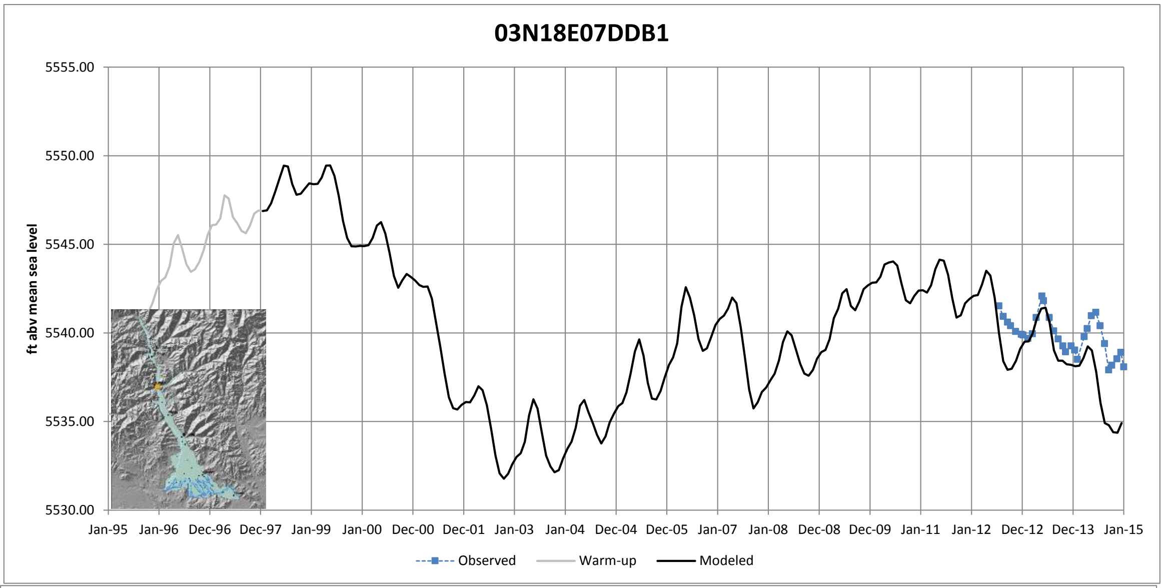
03N18E07DDB1
ft abv mean sea level
5555.00
5550.00
5545.00
5540.00
5535.00
5530.00
Jan-95 Jan-96 Dec-96 Dec-97 Jan-99 Jan-00 Dec-00 Dec-01 Jan-03 Jan-04 Dec-04 Dec-05 Jan-07 Jan-08 Dec-08 Dec-09 Jan-11 Jan-12 Dec-12 Dec-13 Jan-15
Observed
Warm-up
Modeled

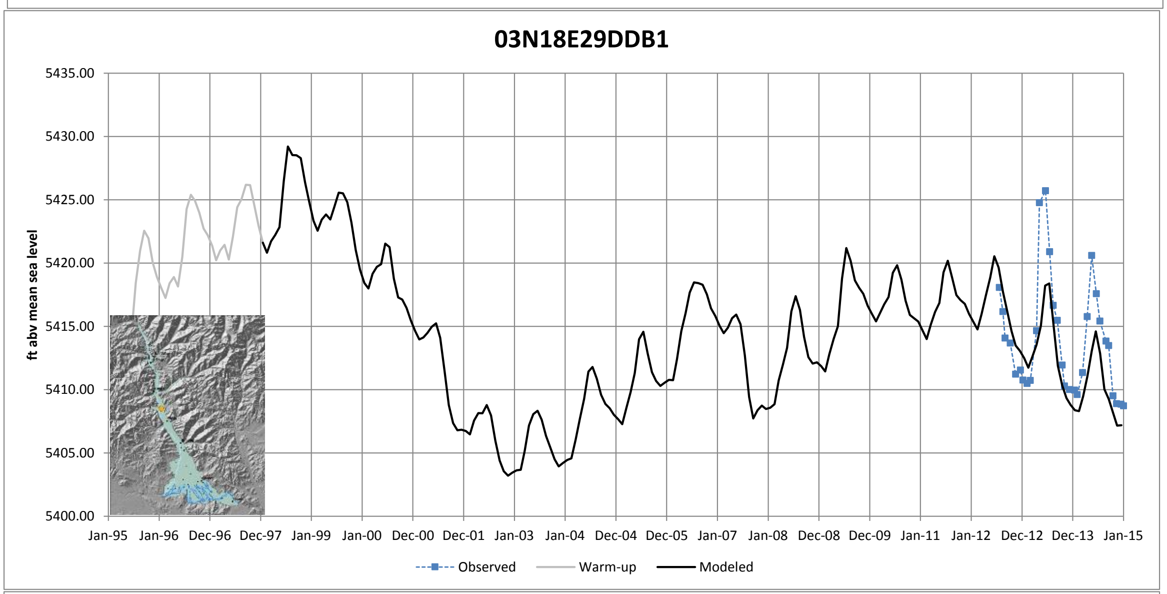
03N18E29DDB1
ft abv mean sea level
5435.00
5430.00
5425.00
5420.00
5415.00
5410.00
5405.00
5400.00
Jan-95 Jan-96 Dec-96 Dec-97 Jan-99 Jan-00 Dec-00 Dec-01 Jan-03 Jan-04 Dec-04 Dec-05 Jan-07 Jan-08 Dec-08 Dec-09 Jan-11 Jan-12 Dec-12 Dec-13 Jan-15
Observed
Warm-up
Modeled

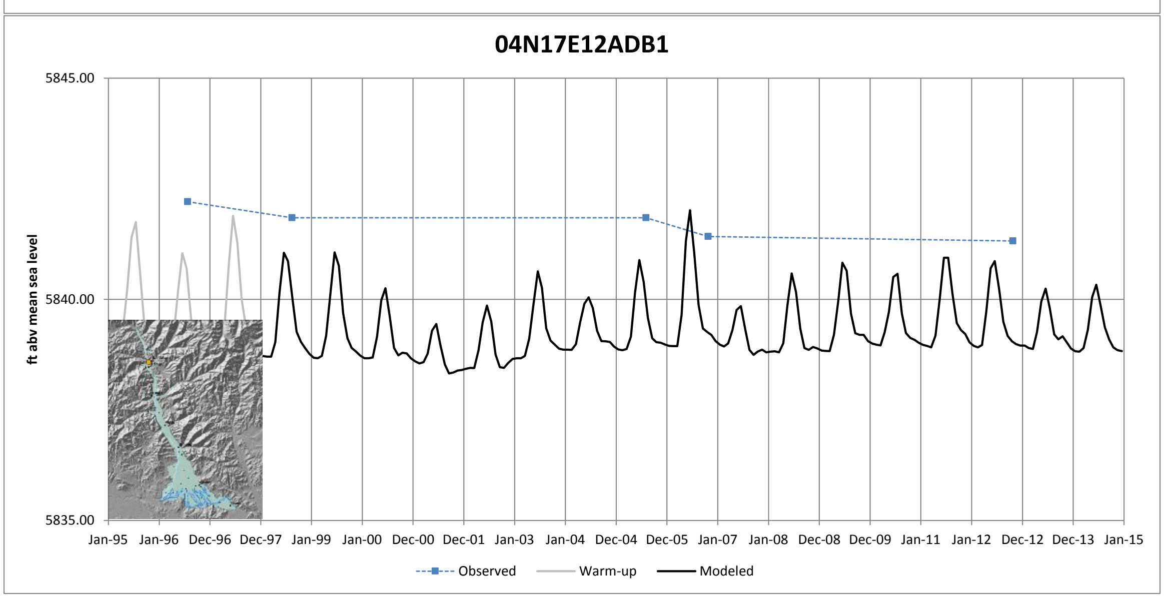
04N17E12ADB1
ft abv mean sea level
5845.00
5840.00
5835.00
Jan-95 Jan-96 Dec-96 Dec-97 Jan-99 Jan-00 Dec-00 Dec-01 Jan-03 Jan-04 Dec-04 Dec-05 Jan-07 Jan-08 Dec-08 Dec-09 Jan-11 Jan-12 Dec-12 Dec-13 Jan-15
Observed
Warm-up
Modeled

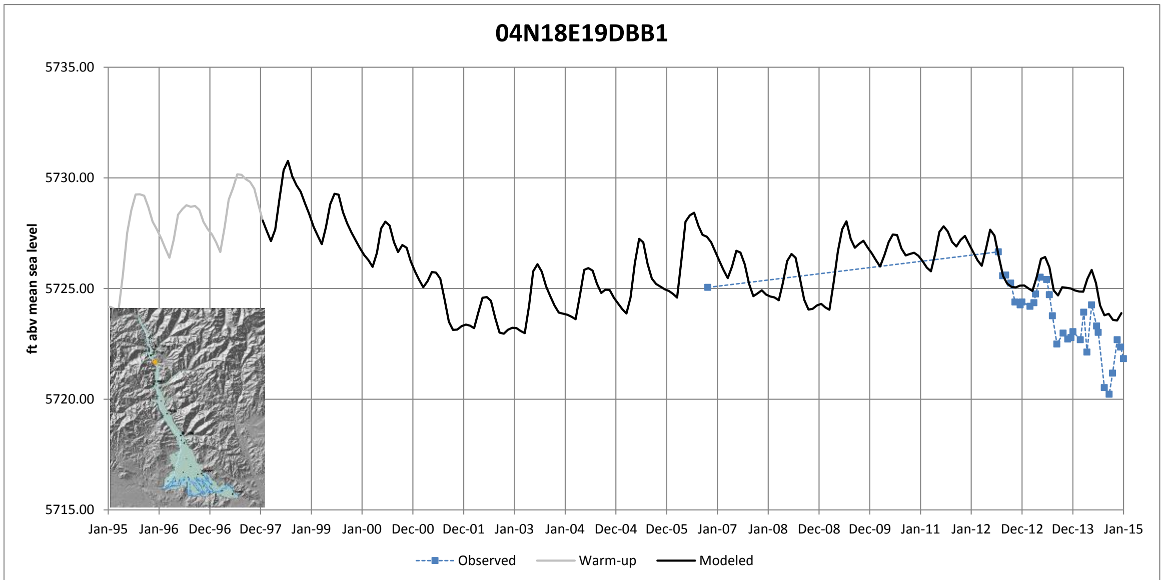
04N18E19DBB1
5735.00
5730.00
5725.00
5720.00
5715.00
ft abv mean sea level
Jan-95
Jan-96
Dec-96
Dec-97
Jan-99
Jan-00
Dec-00
Dec-01
Jan-03
Jan-04
Dec-04
Dec-05
Jan-07
Jan-08
Dec-08
Dec-09
Jan-11
Jan-12
Dec-12
Dec-13
Jan-15
Observed
Warm-up
Modeled

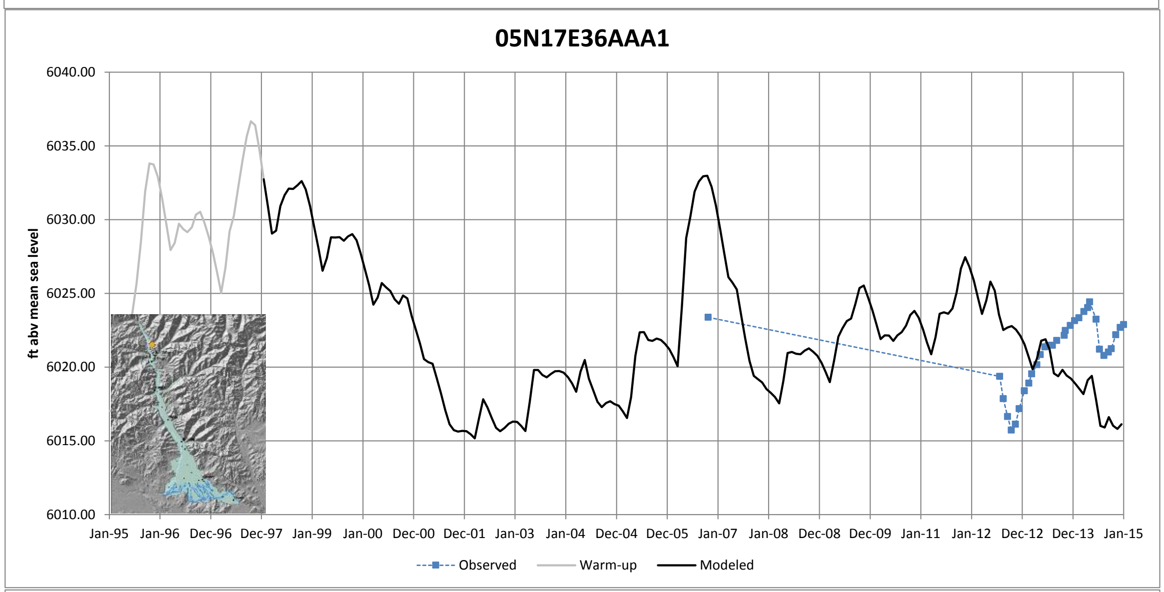
05N17E36AAA1
6040.00
6035.00
6030.00
6025.00
6020.00
6015.00
6010.00
ft abv mean sea level
Jan-95
Jan-96
Dec-96
Dec-97
Jan-99
Jan-00
Dec-00
Dec-01
Jan-03
Jan-04
Dec-04
Dec-05
Jan-07
Jan-08
Dec-08
Dec-09
Jan-11
Jan-12
Dec-12
Dec-13
Jan-15
Observed
Warm-up
Modeled

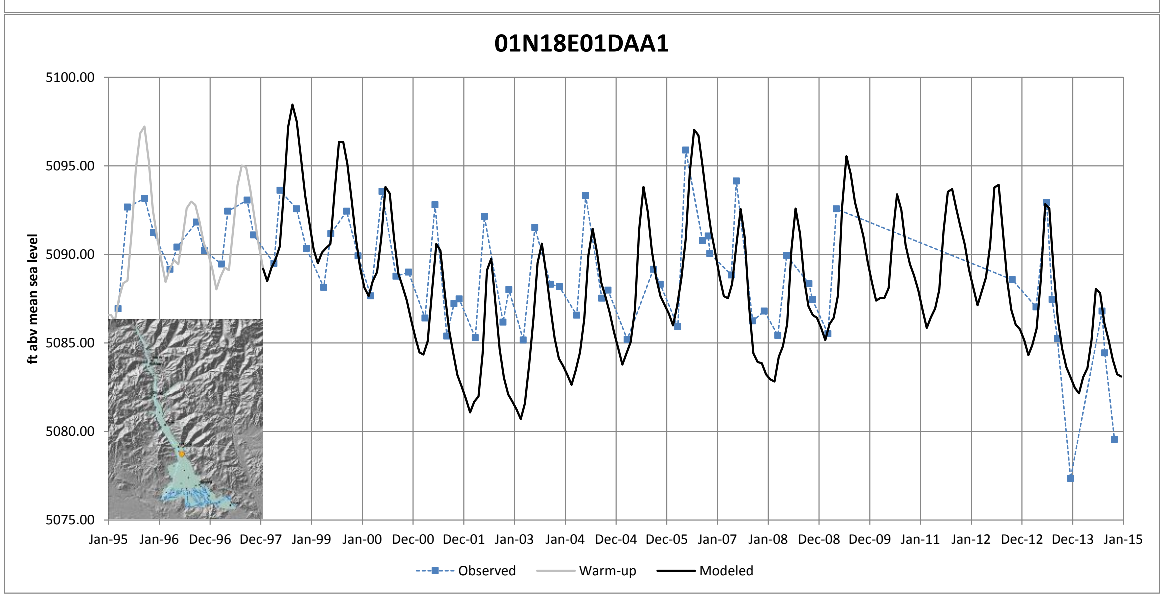
01N18E01DAA1
5100.00
5095.00
5090.00
5085.00
5080.00
5075.00
ft abv mean sea level
Jan-95
Jan-96
Dec-96
Dec-97
Jan-99
Jan-00
Dec-00
Dec-01
Jan-03
Jan-04
Dec-04
Dec-05
Jan-07
Jan-08
Dec-08
Dec-09
Jan-11
Jan-12
Dec-12
Dec-13
Jan-15
Observed
Warm-up
Modeled

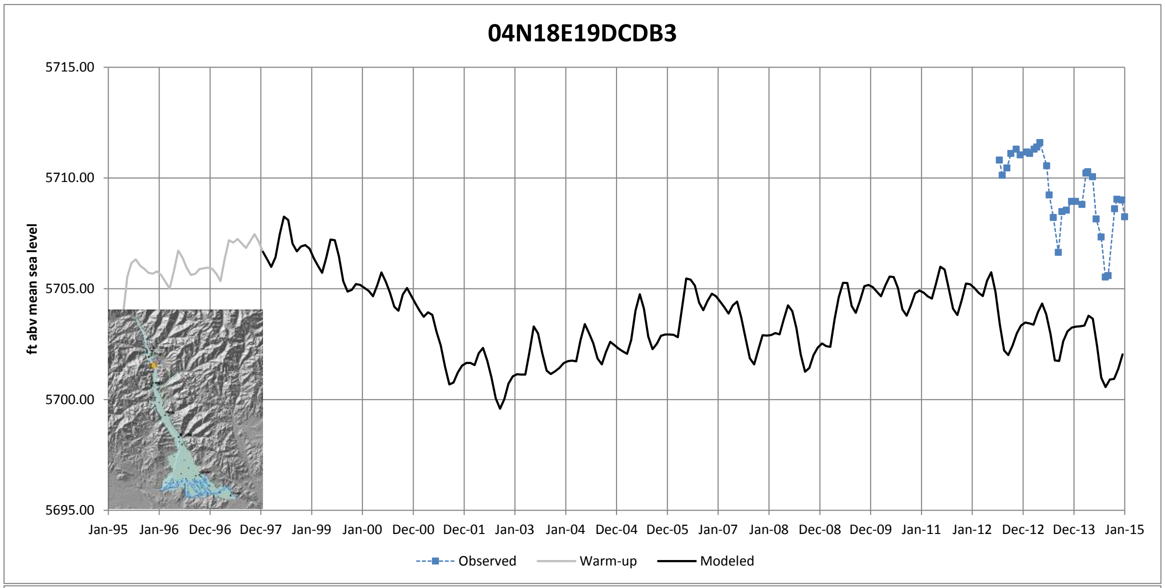
04N18E19DCDB3
ft abv mean sea level
5715.00
5710.00
5705.00
5700.00
5695.00
Jan-95
Jan-96
Dec-96
Dec-97
Jan-99
Jan-00
Dec-00
Dec-01
Jan-03
Jan-04
Dec-04
Dec-05
Jan-07
Jan-08
Dec-08
Dec-09
Jan-11
Jan-12
Dec-12
Dec-13
Jan-15
Observed
Warm-up
Modeled

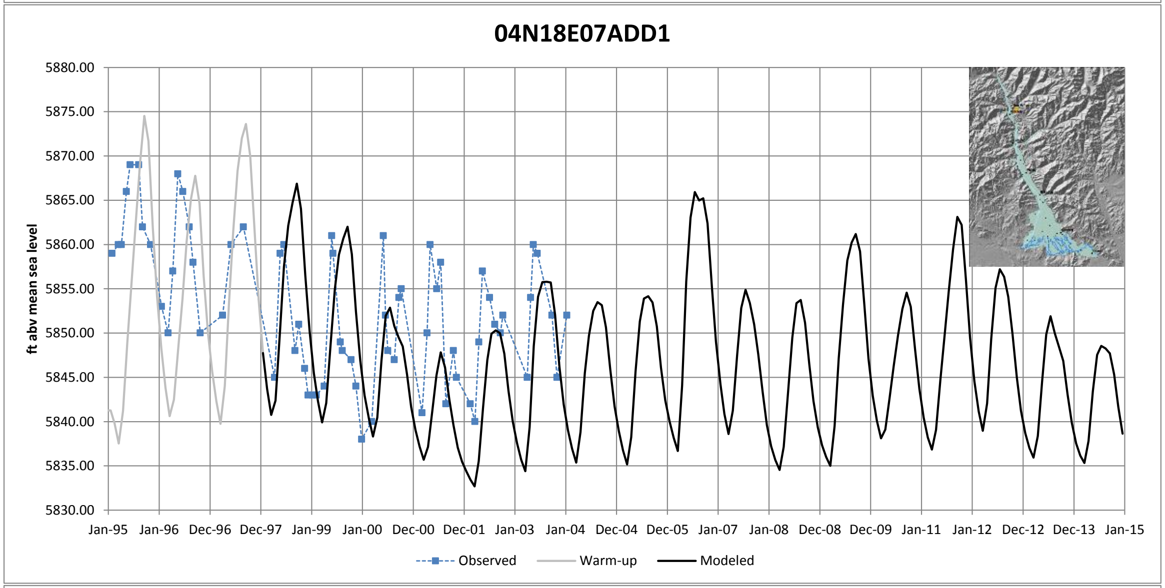
04N18E07ADD1
ft abv mean sea level
5880.00
5875.00
5870.00
5865.00
5860.00
5855.00
5850.00
5845.00
5840.00
5835.00
5830.00
Jan-95
Jan-96
Dec-96
Dec-97
Jan-99
Jan-00
Dec-00
Dec-01
Jan-03
Jan-04
Dec-04
Dec-05
Jan-07
Jan-08
Dec-08
Dec-09
Jan-11
Jan-12
Dec-12
Dec-13
Jan-15
Observed
Warm-up
Modeled

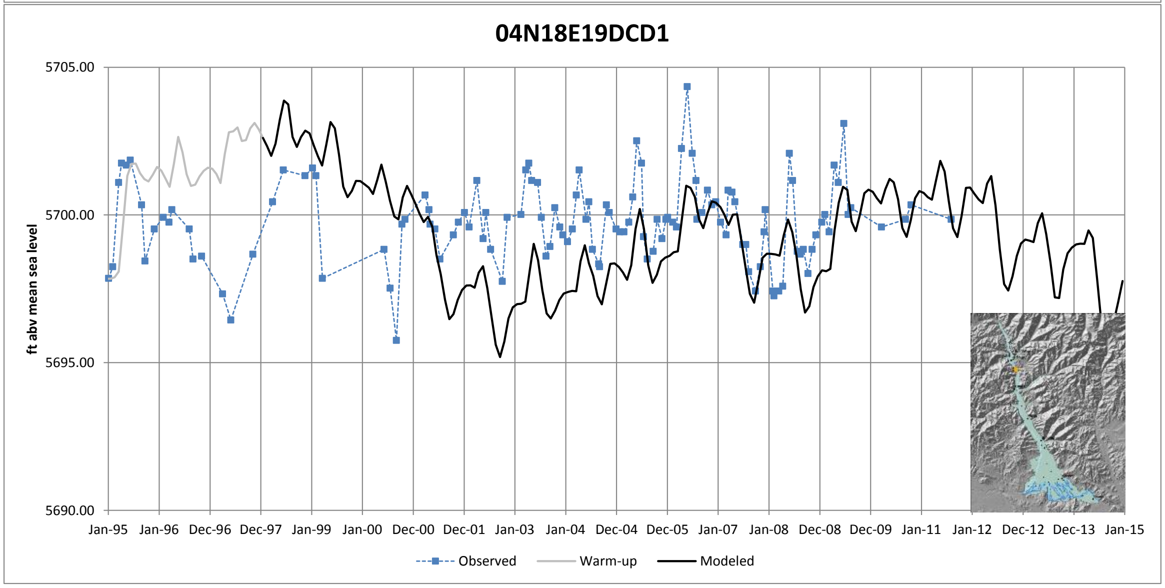
04N18E19DCD1
ft abv mean sea level
5705.00
5700.00
5695.00
5690.00
Jan-95
Jan-96
Dec-96
Dec-97
Jan-99
Jan-00
Dec-00
Dec-01
Jan-03
Jan-04
Dec-04
Dec-05
Jan-07
Jan-08
Dec-08
Dec-09
Jan-11
Jan-12
Dec-12
Dec-13
Jan-15
Observed
Warm-up
Modeled

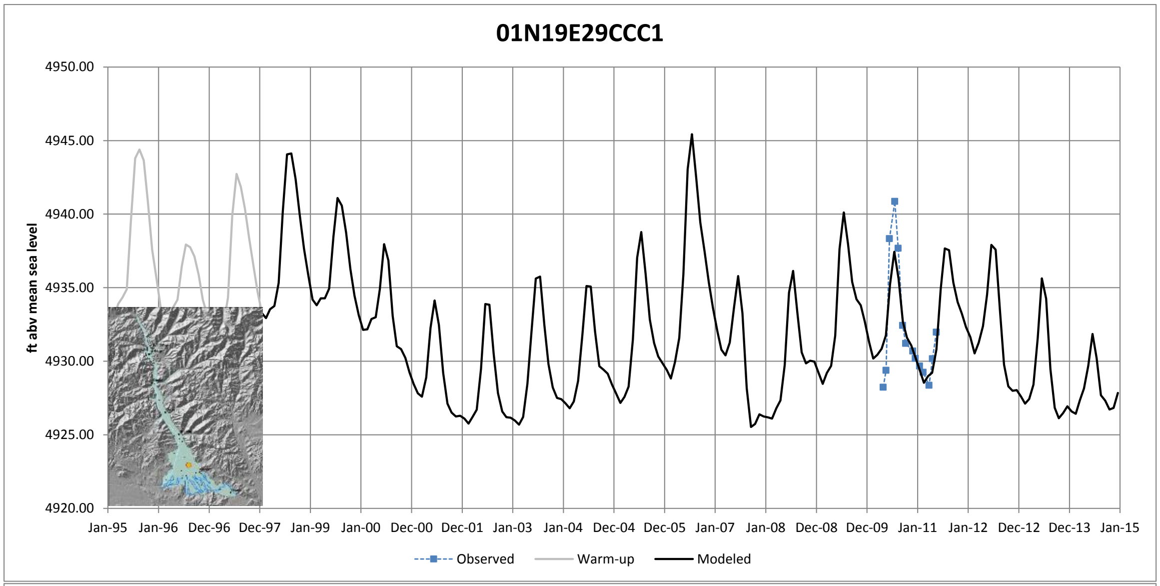
01N19E29CCC1
ft abv mean sea level
4950.00
4945.00
4940.00
4935.00
4930.00
4925.00
4920.00
Jan-95
Jan-96
Dec-96
Dec-97
Jan-99
Jan-00
Dec-00
Dec-01
Jan-03
Jan-04
Dec-04
Dec-05
Jan-07
Jan-08
Dec-08
Dec-09
Jan-11
Jan-12
Dec-12
Dec-13
Jan-15
Observed
Warm-up
Modeled

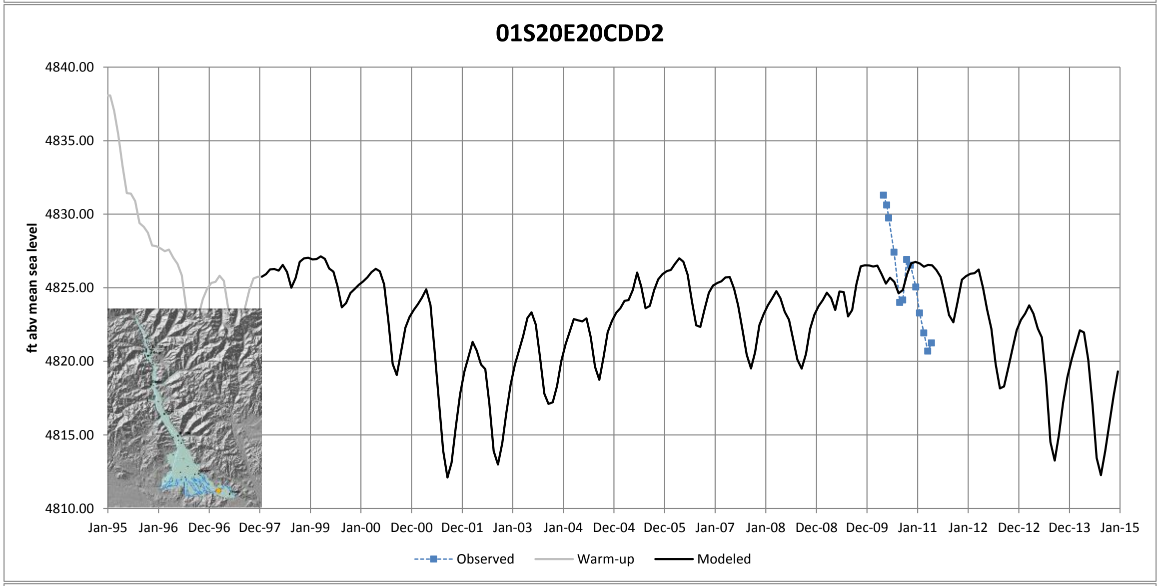
01S20E20CDD2
ft abv mean sea level
4840.00
4835.00
4830.00
4825.00
4820.00
4815.00
4810.00
Jan-95
Jan-96
Dec-96
Dec-97
Jan-99
Jan-00
Dec-00
Dec-01
Jan-03
Jan-04
Dec-04
Dec-05
Jan-07
Jan-08
Dec-08
Dec-09
Jan-11
Jan-12
Dec-12
Dec-13
Jan-15
Observed
Warm-up
Modeled

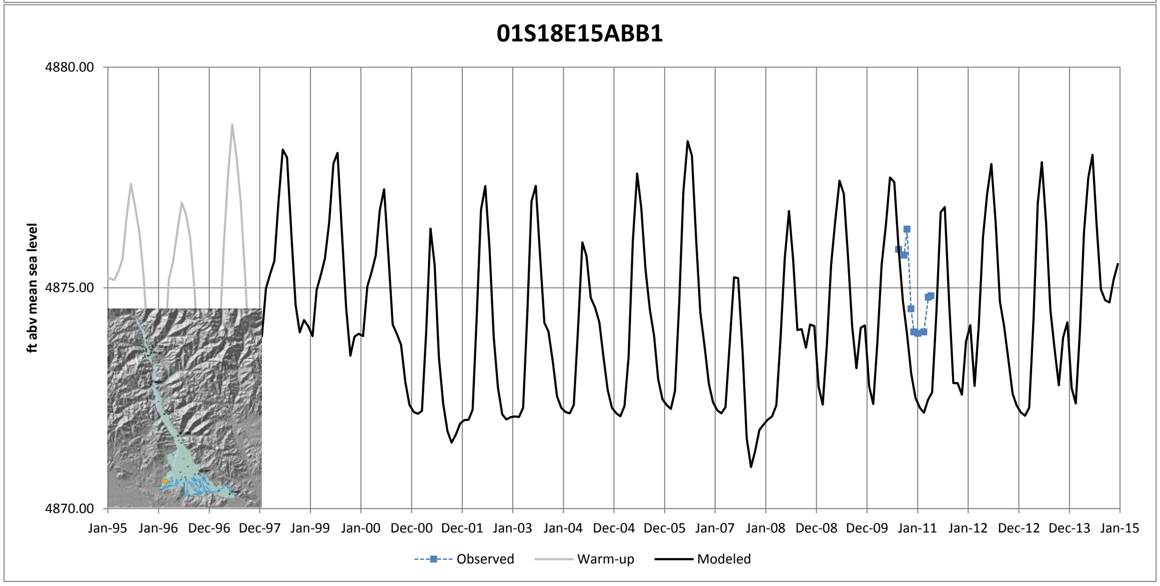
01S18E15ABB1
ft abv mean sea level
4880.00
4875.00
4870.00
Jan-95
Jan-96
Dec-96
Dec-97
Jan-99
Jan-00
Dec-00
Dec-01
Jan-03
Jan-04
Dec-04
Dec-05
Jan-07
Jan-08
Dec-08
Dec-09
Jan-11
Jan-12
Dec-12
Dec-13
Jan-15
Observed
Warm-up
Modeled

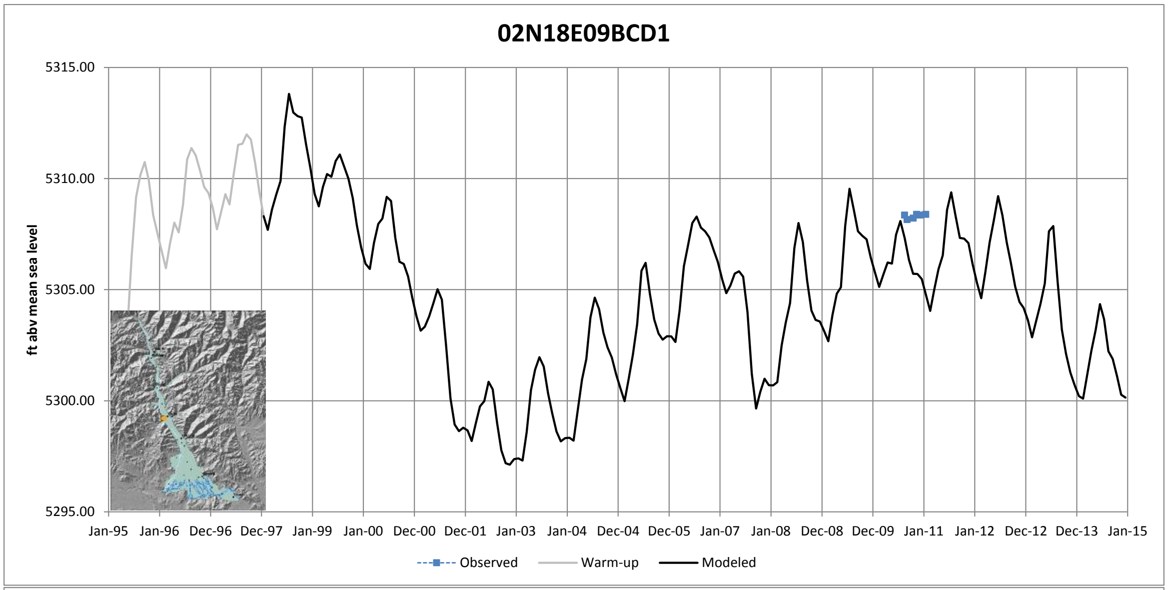
02N18E09BCD1
5315.00
5310.00
5305.00
5300.00
5295.00
ft abv mean sea level
Jan-95 Jan-96 Dec-96 Dec-97 Jan-99 Jan-00 Dec-00 Dec-01 Jan-03 Jan-04 Dec-04 Dec-05 Jan-07 Jan-08 Dec-08 Dec-09 Jan-11 Jan-12 Dec-12 Dec-13 Jan-15
Observed
Warm-up
Modeled

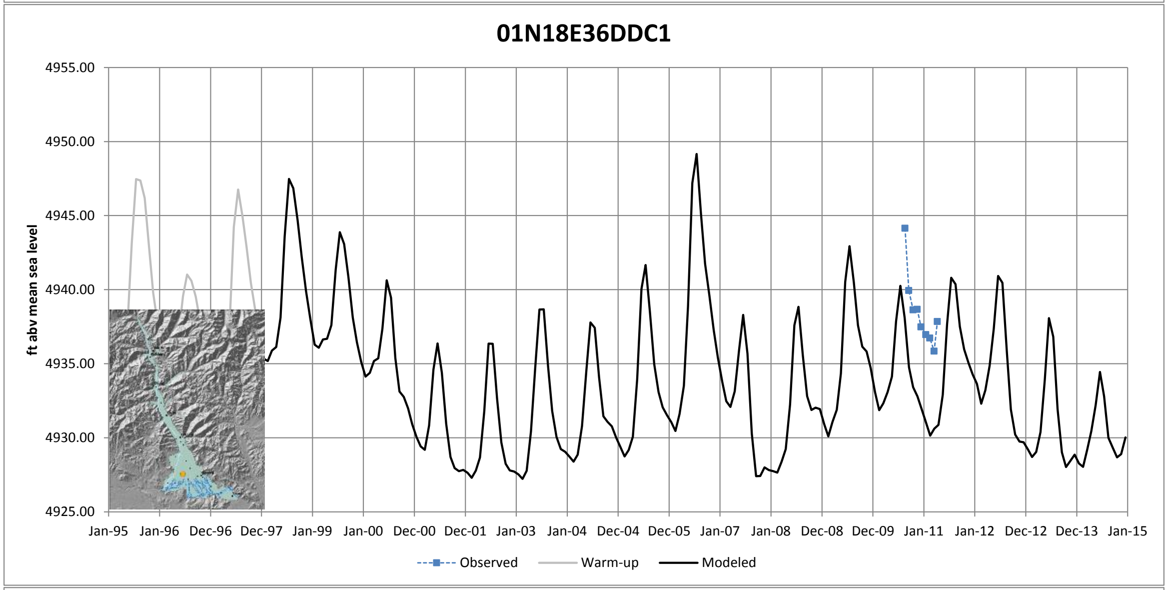
01N18E36DDC1
4955.00
4950.00
4945.00
4940.00
4935.00
4930.00
4925.00
ft abv mean sea level
Jan-95 Jan-96 Dec-96 Dec-97 Jan-99 Jan-00 Dec-00 Dec-01 Jan-03 Jan-04 Dec-04 Dec-05 Jan-07 Jan-08 Dec-08 Dec-09 Jan-11 Jan-12 Dec-12 Dec-13 Jan-15
Observed
Warm-up
Modeled

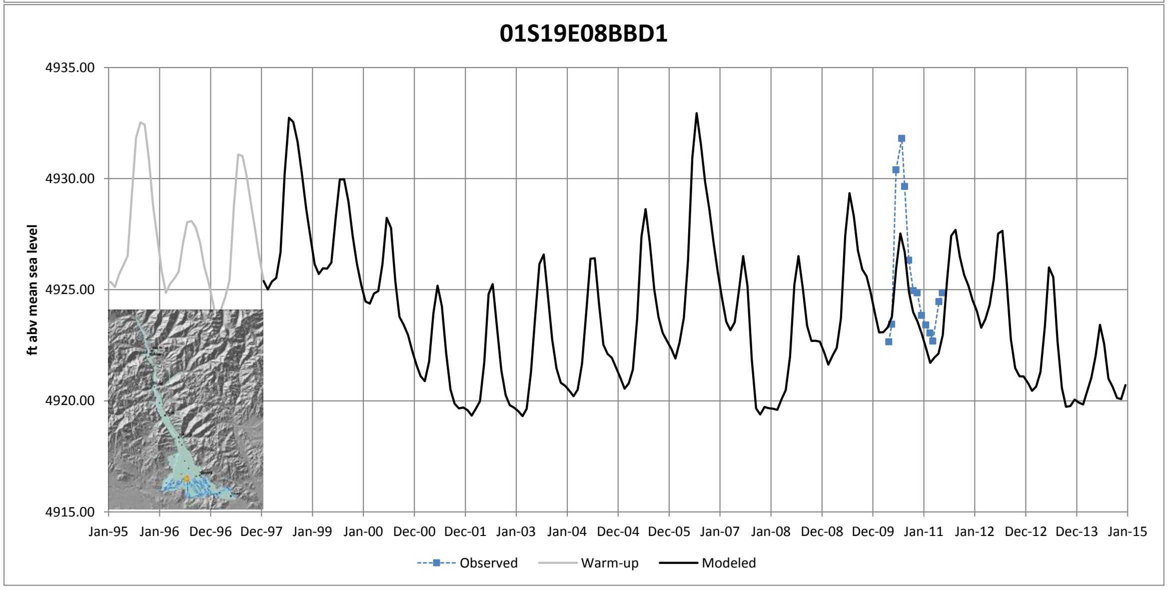
01S19E08BBD1
4935.00
4930.00
4925.00
4920.00
4915.00
ft abv mean sea level
Jan-95 Jan-96 Dec-96 Dec-97 Jan-99 Jan-00 Dec-00 Dec-01 Jan-03 Jan-04 Dec-04 Dec-05 Jan-07 Jan-08 Dec-08 Dec-09 Jan-11 Jan-12 Dec-12 Dec-13 Jan-15
Observed
Warm-up
Modeled

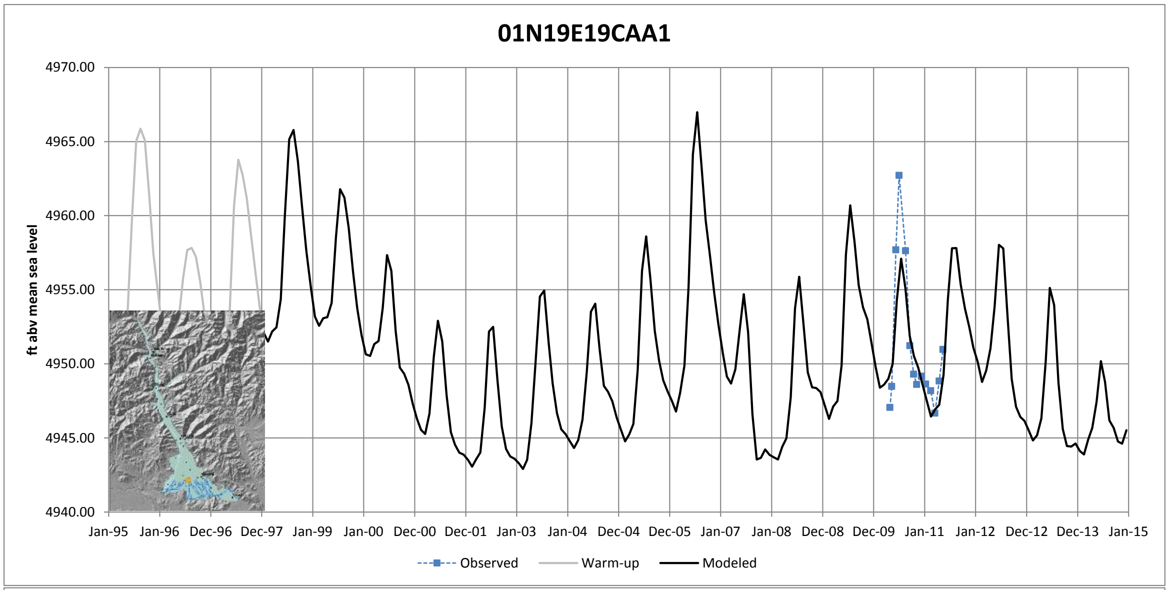

01N19E19CAA1
ft abv mean sea level
4970.00
4965.00
4960.00
4955.00
4950.00
4945.00
4940.00
Jan-95 Jan-96 Dec-96 Dec-97 Jan-99 Jan-00 Dec-00 Dec-01 Jan-03 Jan-04 Dec-04 Dec-05 Jan-07 Jan-08 Dec-08 Dec-09 Jan-11 Jan-12 Dec-12 Dec-13 Jan-15
Observed
Warm-up
Modeled

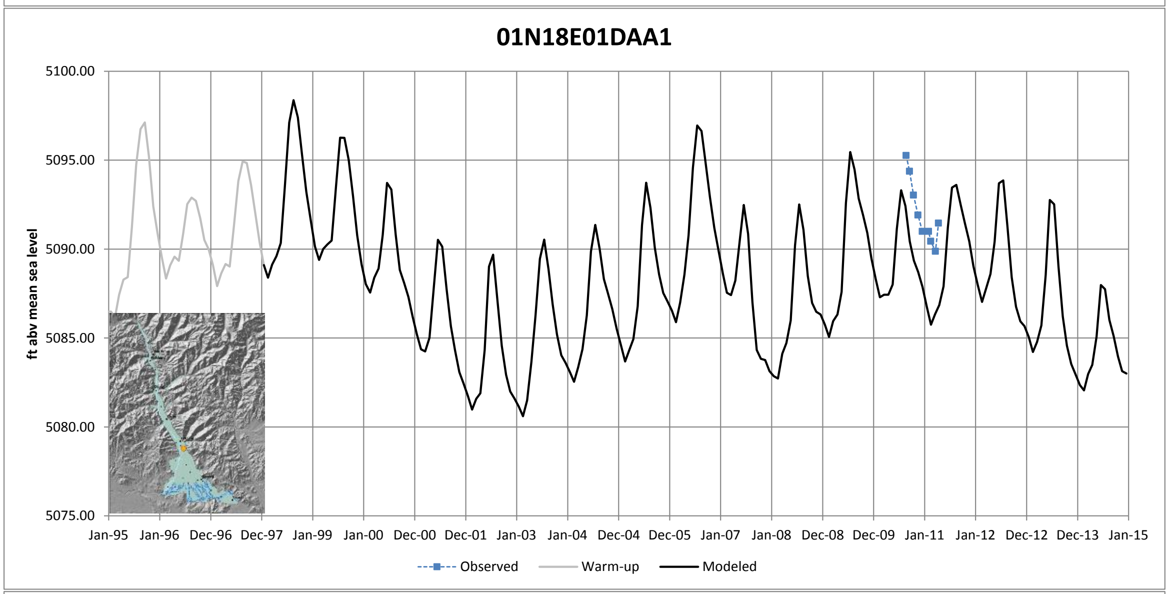

01N18E01DAA1
ft abv mean sea level
5100.00
5095.00
5090.00
5085.00
5080.00
5075.00
Jan-95 Jan-96 Dec-96 Dec-97 Jan-99 Jan-00 Dec-00 Dec-01 Jan-03 Jan-04 Dec-04 Dec-05 Jan-07 Jan-08 Dec-08 Dec-09 Jan-11 Jan-12 Dec-12 Dec-13 Jan-15
Observed
Warm-up
Modeled

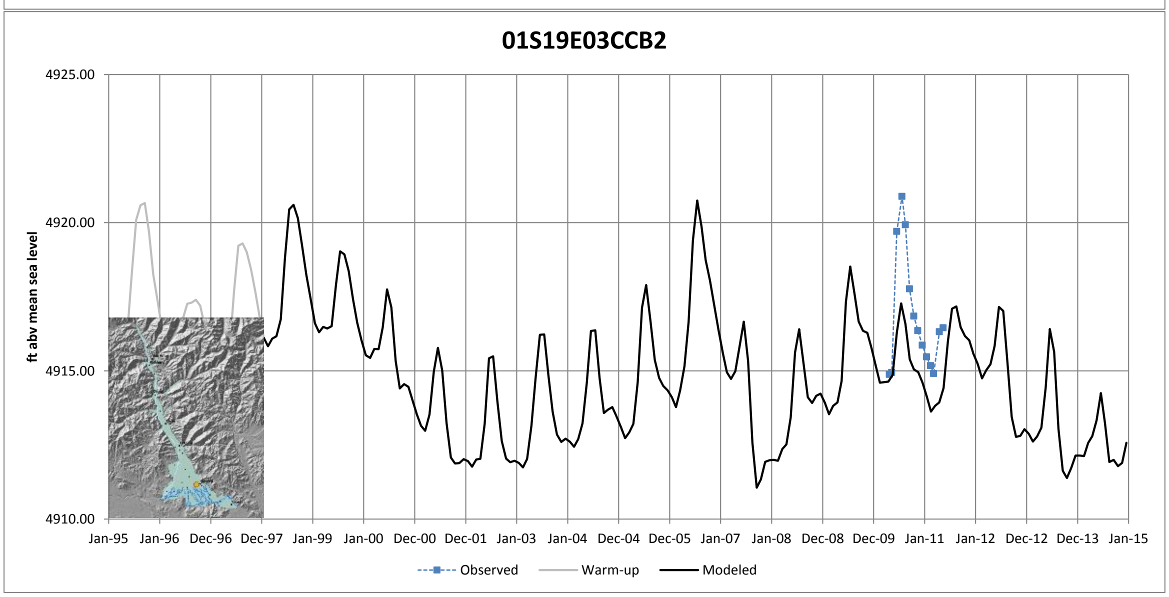

01S19E03CCB2
ft abv mean sea level
4925.00
4920.00
4915.00
4910.00
Jan-95 Jan-96 Dec-96 Dec-97 Jan-99 Jan-00 Dec-00 Dec-01 Jan-03 Jan-04 Dec-04 Dec-05 Jan-07 Jan-08 Dec-08 Dec-09 Jan-11 Jan-12 Dec-12 Dec-13 Jan-15
Observed
Warm-up
Modeled

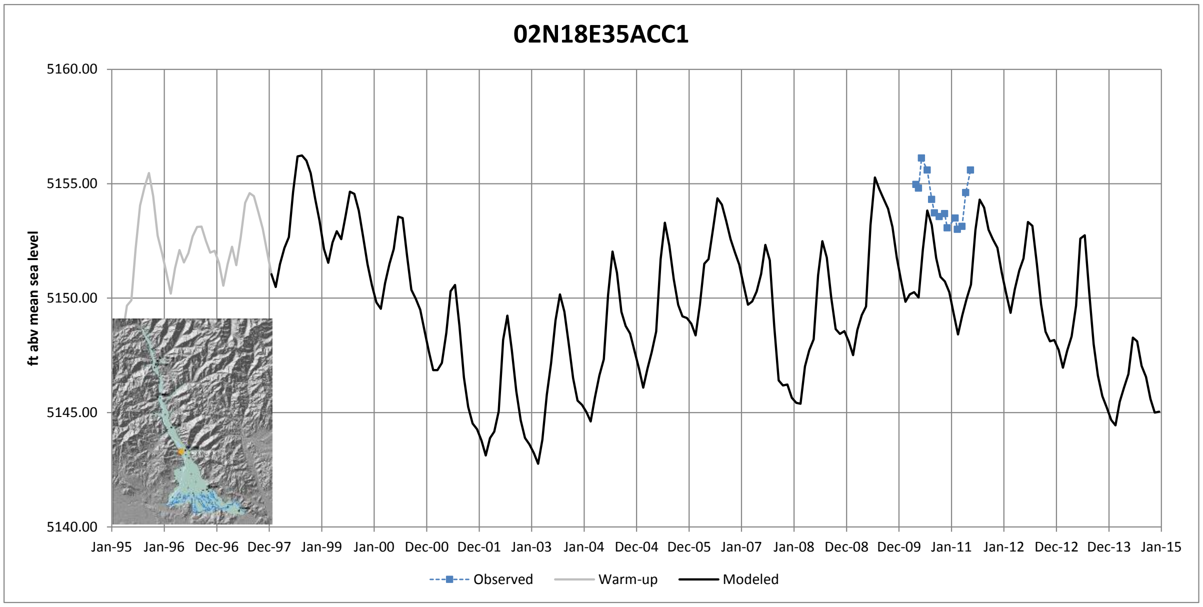
02N18E35ACC1
5160.00
5155.00
5150.00
5145.00
5140.00
ft abv mean sea level
Jan-95
Jan-96
Dec-96
Dec-97
Jan-99
Jan-00
Dec-00
Dec-01
Jan-03
Jan-04
Dec-04
Dec-05
Jan-07
Jan-08
Dec-08
Dec-09
Jan-11
Jan-12
Dec-12
Dec-13
Jan-15
Observed
Warm-up
Modeled